


Links between the Microvascular and Neural Systems: Multicellular Interactions during Angiogenesis

A DISSERTATION
SUBMITTED ON THE 4th DAY OF APRIL, 2013
TO THE DEPARTMENT OF BIOMEDICAL ENGINEERING
OF THE SCHOOL OF SCIENCE AND ENGINEERING
AT TULANE UNIVERSITY
IN PARTIAL FULFILLMENT OF THE REQUIREMENTS
FOR THE DEGREE OF
DOCTOR OF PHILOSOPHY
BY


PETER C. STAPOR

APPROVED: 
WALTER L. MURFEE, PHD


DONALD P. GAVAR, PHD


TABASSAM AHSAN, PHD


JEROME W. BRESLIN, PHD

ABSTRACT

Angiogenesis, defined as the growth of new blood vessels from existing vasculature, is essential for normal physiological function and tissue homeostasis, and its dysfunction is a common denominator in multiple disease pathologies. In order to fully understand angiogenesis, we must probe the multicellular interactions among cells within the microvasculature, and relationships with other systems such as the nervous system. The aims of this study were to 1) determine the spatiotemporal relationship between angiogenesis and neurovascular alignment; 2) determine whether class III β -tubulin is a functional marker of perivascular cells during angiogenesis; 3) develop an *in vitro* culture model using the adult rat mesentery to investigate multicellular interactions during angiogenesis within intact microvascular networks.

Nerves influence vascular patterning during development by paracrine signaling of factors which stimulate angiogenesis. However, their role during angiogenesis in the adult remains unclear. The goal of Aim 1 was to determine whether nerves are involved in angiogenesis in the adult by quantifying the spatiotemporal relationship between microvasculature and nerves across the hierarchy of adult rat mesentery microvascular networks over the time course of angiogenesis.


Pericytes, which participate in angiogenesis and are critical for stabilization of new vessels, are difficult to identify because of their heterogeneous phenotypes and roles in microvascular remodeling. Immunolabeling in Aim 1 revealed that pericytes express the neural marker, class III β -tubulin. The goal of Aim 2 was to determine whether class III β -tubulin is a functional marker of angiogenic pericytes. Its expression pattern across the microvascular hierarchy was characterized over the time course of angiogenesis. Then, class III β -tubulin expression by human vascular pericytes was inhibited *in vitro* with siRNA to elucidate its function in proliferation and migration.

The importance of class III β -tubulin expression during angiogenesis remains unclear because current experimental methods to investigate pericyte-endothelial cell interactions are limited by insufficient spatial resolution, unknown delivery efficacy and lack of local environmental control. The goal of Aim 3 was to establish a model to investigate multicellular interactions within intact microvascular networks. To establish the model, the angiogenic response to growth factors and function-blocking antibodies targeting pericytes was quantified in cultured rat mesentery windows.

Links between the Microvascular and Neural Systems: Multicellular Interactions during Angiogenesis

A DISSERTATION
SUBMITTED ON THE 4th DAY OF APRIL, 2013
TO THE DEPARTMENT OF BIOMEDICAL ENGINEERING
OF THE SCHOOL OF SCIENCE AND ENGINEERING
AT TULANE UNIVERSITY
IN PARTIAL FULFILLMENT OF THE REQUIREMENTS
FOR THE DEGREE OF
DOCTOR OF PHILOSOPHY
BY


PETER C. STAPOR

APPROVED: 
WALTER L. MURFEE, PHD


DONALD P. GAVAR, PHD


TABASSAM AHSAN, PHD


JEROME W. BRESLIN, PHD

ACKNOWLEDGEMENTS

I would like to thank the Tulane University Department of Biomedical Engineering for giving me the opportunity to pursue a doctoral degree, and resources to undertake this research. I would especially like to thank Dr. Walter Lee Murfee for his guidance in and out of the laboratory over the past five years. He was the reason I came to Tulane University, the best mentor I could have asked for and has become a true friend. I want to thank all the members of the Microvascular Dynamics Laboratory over my residence including Ming Yang, Jennifer Robichaux, Rick Sweat, Sadegh Azimi, Molly Kelly-Goss, Hudson Chien, Kate Schimmer, Erica Winterer, Liz Townsend and Oliva Bigazzi. It was a pleasure working with you all, and I always had a lot of fun in the lab. Additionally, I want to recognize and thank those who have given me support outside the Murfee Lab including Dr. Donald Gaver, Dr. Taby Ahsan, Dr. Damir Khismatullin, Dr. Sergey Shevkoplyas, Dr. Dave Rice, Dr. Jerry Breslin, Dr. Weixong Wang, Dr. Michael Moore, Dr. Mic Dancisak, Dr. Ali Betancourt, Dr. Shayn Peirce-Cottler, Dr. Becky Worthylake, Megan Ohar, Lorrie McGinley, Cindy Stewart, Derek Dashti, Russ Wolfe, Emma Pineda and Carol Chen. Finally, I want to thank Kristen, my parents, my sister and my brothers for their unconditional love and support throughout my life and as I embark on another journey.

TABLE OF CONTENTS

LIST OF FIGURES	vi
CHAPTER 1: BACKGROUND	1
1.1 Introduction	1
1.2 The Microcirculation in Health and Disease	4
1.2.1 Overview of the Microcirculation	4
1.2.2 Angiogenesis	6
1.3 Microvascular and Neural Links	10
1.3.1 Anatomical	10
1.3.2 Growth Mechanisms	11
1.4 Pericytes in the Microcirculation	13
1.4.1 Function in the Microvasculature	13
1.4.2 Function during Angiogenesis	14
1.4.3 Heterogeneous Phenotypes	15
1.4.4 Neural Phenotypes	16
1.5 Models for Studying Angiogenesis	18
1.5.1 In Vitro	18
1.5.2 The Adult Rat Mesentery as an In Vivo Model of Angiogenesis	19
1.6 Specific Aims	21
CHAPTER 2: METHODS AND MATERIALS	25
2.1 Spatiotemporal Relationship between Angiogenesis and Neurovascular Alignment	25
2.1.1 Mast Cell Degranulation Model	25
2.1.2 Mesentery Exteriorization Model	26
2.1.3 Chronic Hypoxia Model	26
2.1.4 Immunohistochemistry	27
2.1.5 Imaging	28
2.1.6 Quantification of Angiogenesis and Neurovascular Alignment	28
2.1.7 Statistical Analysis	29

2.2	Class III β-Tubulin as a Functional Marker of Perivascular Cells during Angiogenesis	30
2.2.1	Stimulation of Angiogenesis	30
2.2.2	Alternative Models of Angiogenesis	30
2.2.3	Tissue Immunohistochemistry	31
2.2.4	Tissue Imaging	32
2.2.5	Quantification of Angiogenesis and Perivascular Cell Expression of Class III β -Tubulin	32
2.2.6	Statistical Analysis	33
2.2.7	Cell Culture	33
2.2.8	Inhibition of Class III β -Tubulin by siRNA	33
2.2.9	Proliferation Assay	34
2.2.10	Migration Assay	34
2.2.11	Cell Immunohistochemistry	35
2.2.12	Cell Imaging	35
2.2.13	Statistical Analysis	35
2.3	The Adult Rat Mesentery as a Model for Multicellular and Multisystem Interactions during Angiogenesis	37
2.3.1	Tissue Culture Method	37
2.3.2	Stimulation of Angiogenesis and NG2 Inhibition	38
2.3.3	Immunohistochemistry	39
2.3.4	Imaging	41
2.3.5	Quantification of NG2 Expression	41
2.3.6	Quantification of Angiogenesis	42
2.3.7	Quantification of Lymphatic / Blood Endothelial Cell Connections	42
2.3.8	Statistical Analysis	43
CHAPTER 3:	RESULTS	44
3.1	Spatiotemporal Relationship between Angiogenesis and Neurovascular Alignment	44
3.1.1	Neurovascular Alignment across the Microvascular Hierarchy	44
3.1.2	Neurovascular Alignment during Angiogenesis	46
3.2	Class III β-Tubulin as a Functional Marker of Perivascular Cells during Angiogenesis	52
3.2.1	Vascular Expression of Class III β -Tubulin	52
3.2.2	Expression of Class III β -Tubulin during Angiogenesis	53
3.2.3	Effects of Class III β -Tubulin Inhibition on Pericyte Proliferation and Migration	54
3.3	The Adult Rat Mesentery as a Model for Multicellular and Multisystem Interactions during Angiogenesis	62

3.3.1 Assessment of Microvascular Viability, Morphology and Phenotype	62
3.3.2 Stimulation of Capillary Sprouting at Specific Vessel Locations	64
3.3.3 Regulation of Capillary Sprouting by Endothelial Cell-Pericyte Interactions	64
3.3.4 Modulation of Lymphatic/Blood Endothelial Cell Interactions during Angiogenesis	65
CHAPTER 4: DISCUSSION	73
4.1 Spatiotemporal Relationship between Angiogenesis and Neurovascular Alignment	73
4.1.1 Limitations	77
4.2 Class III β -Tubulin as a Functional Marker of Perivascular Cells during Angiogenesis	79
4.2.1 Limitations	85
4.3 The Adult Rat Mesentery as a Model for Multicellular and Multisystem Interactions during Angiogenesis	87
4.3.1 Limitations	93
CHAPTER 5: CONCLUSIONS	94
CHAPTER 6: FUTURE STUDIES	96
6.1 Spatiotemporal Relationship between Angiogenesis and Neurovascular Alignment	97
6.2 Class III β -Tubulin as a Functional Marker of Perivascular Cells during Angiogenesis	99
6.3 The Adult Rat Mesentery as a Model for Multicellular and Multisystem Interactions during Angiogenesis	101
CHAPTER 7: REFERENCES	103
BIOGRAPHY	112

LIST OF FIGURES

Figure 1.	Multicellular and Multisystem Interactions during Angiogenesis.	7
Figure 2.	Modes of Angiogenesis.	8
Figure 3.	Neurovascular Alignment.	10
Figure 4.	NG2 Expression by Pericytes.	17
Figure 5.	The Aortic Ring Assay.	18
Figure 6.	Neurovascular Alignment in Adult Rat Mesentery Window Microvascular Networks.	44
Figure 7.	Neurovascular Alignment along Capillary Sprout.	45
Figure 8.	Neurovascular Alignment over 30 Days.	46
Figure 9.	Class III β -Tubulin Co-Labels with Tyrosine Hydroxylase.	47
Figure 10.	Quantification of Vessel Density.	49
Figure 11.	Quantification of Neurovascular Alignment.	50
Figure 12.	Neurovascular Alignment in Alternative Models of Angiogenesis.	51
Figure 13.	Class III β -Tubulin Expression during Angiogenesis.	54
Figure 14.	Class III β -Tubulin Expression by Pericytes.	56
Figure 15.	Quantification of Class III β -Tubulin Expression by Pericytes.	57

Figure 16. Class III β -Tubulin Expression in Alternative Models of Angiogenesis.	58
Figure 17. Human Pericyte Expression of Class III β -Tubulin.	59
Figure 18. Quantification of Proliferation.	60
Figure 19. Quantification of Migration.	61
Figure 20. Mural Cells in the Mesentery Culture Model.	63
Figure 21. Lymphatics and Nerves in the Mesentery Culture Model.	66
Figure 22. Cell Viability in the Mesentery Culture Model.	67
Figure 23. Angiogenesis in the Mesentery Culture Model.	68
Figure 24. Quantification of Angiogenesis.	69
Figure 25. NG2 Targeting.	70
Figure 26. Lymphatic Connections in the Mesentery Culture Model.	71
Figure 27. Lymphangiogenesis in the Mesentery Culture Model.	72

CHAPTER 1: BACKGROUND

1.1 Introduction

Microvascular remodeling is essential for normal physiological function and tissue homeostasis, and its dysfunction is a common denominator in multiple disease pathologies including cancer, diabetic retinopathy and hypertension. Accordingly, the microvasculature has been a target for therapies to treat such diseases, and its understanding is critical for the advancement of tissue engineering. Success requires a better comprehension of microvascular remodeling processes, including angiogenesis, defined as the growth of new vessels from existing vessels, and arteriogenesis, defined as capillary acquisition of perivascular cells. Central to these processes are vascular cell types, such as endothelial cells and pericytes, and their interactions with other systems, including the nervous system. Identifying such cellular- and system-level relationships and discerning their functional interplay with the microvasculature is critical to comprehending abnormal microvascular remodeling, and engineering functionalized tissues.

An emerging area of microvascular research focuses on the links between the vascular and nervous systems. Support for the link stems from evidence suggesting that the vascular system co-opted growth mechanisms and cues from the nervous system.

Vascular and neural networks respond to common molecular signals during angiogenesis, and its neural analog, neurogenesis, influence each other's patterns during development,

and share phenotypic characteristics. This dissertation will highlight the links between the vascular and nervous systems at the microvascular level during angiogenesis by 1) characterizing the spatial relationship between microvascular and neural networks during angiogenesis in the adult, 2) identifying class III β -tubulin, typically associated with neural phenotypes, as a functional marker of angiogenic perivascular cells, and 3) establishing the rat mesentery as a tissue culture model for probing cellular- and system-level interactions within intact microvascular networks.

In the first study, we mapped the spatiotemporal dynamics of neurovascular alignment across the hierarchy of adult rat microvascular networks during angiogenesis. Vascular and neural networks have been shown to influence each other's growth patterns during embryonic development through paracrine signaling, as well as respond to the same guidance cues. Since both systems respond to the same signals, their functional interdependence during angiogenesis in adult tissues remains unclear. Characterizing the extent of neurovascular alignment along angiogenic microvascular networks indicates the importance of neural networks in microvascular growth by spatial location along the vessel hierarchy. The spatial location of neurovascular alignment in mesenteric adult microvascular networks indicates the potential for interactions between the systems along arterioles, venules, capillaries and capillary sprouts. Our results are the first to show that neurovascular alignment occurs across all vessel types after angiogenesis has subsided in adult rat mesentery microvascular networks, suggesting that nerves do not play a role in angiogenesis and implicating neurovascular alignment in the vessel maturation process.

In the second part of this study, we identified a neural phenotype as a novel marker of pericytes during angiogenesis, and indicate its functional role in proliferation and migration. While pericytes have been identified as important players in angiogenesis, our understanding of their specific mechanisms of action is limited by a lack of pericyte-specific markers. Recent identification of Neuron Glial Antigen 2 (NG2) as a pericyte marker has highlighted a neurovascular phenotype, and led to its establishment as a functional molecule during angiogenesis. The question of whether other neural phenotypic markers can be used to study perivascular cell function remains. NG2 and class III β -tubulin are both expressed by glial and neural precursor cells in the central nervous system and by nerves in the peripheral nervous system. Our results establish class III β -tubulin as novel marker of angiogenic perivascular cells highlighting another neurovascular phenotype, and implicate its functional role in pericyte proliferation and migration.

The third section of this study establishes a tissue culture model using adult rat mesentery windows to study cellular dynamics within tissues that include intact microvascular, lymphatic and neural networks. A critical barrier to advancing angiogenesis research is our inability to probe specific cellular interactions in a controlled environment, such as those between vascular and neural networks or pericytes and endothelial cells. The rat mesentery culture model provides an *in vitro* platform to study capillary sprouting within intact microvascular networks. Our results validate the rat mesentery culture model as a new tool to investigate pericyte-endothelial cell interactions during angiogenesis and lymphatic-blood endothelial cell interactions.

1.2 The Microcirculation in Health and Disease

1.2.1 Overview of the Microcirculation

The microcirculation consists of the smallest blood vessels in the vascular system including arterioles, capillaries and venules ranging from 5 to 200 μm . Its function is critical to maintaining homeostasis throughout the body. Every organ relies on the cardiovascular system to transport blood to the microcirculation where the exchange of oxygen, water, nutrients, signaling molecules and waste allows normal physiological function. The microvasculature also plays an essential role in immune response and immune cell trafficking to sites of injury and infection. Physiologically specialized to suit each tissue, the microcirculation is the marketplace for cardiovascular transactions with the body, and facilitates non-neuronal communication between systems [1].

The microvasculature is a hierarchical structure composed of arterioles, capillaries and venules, which each have unique features and behaviors reflective of their functions. Arterioles feed microvascular networks and maintain normal blood pressure in response to fluctuations in metabolic demand. For example, during exercise oxygen consumption by muscle causes arterioles to dilate, which promotes blood flow and muscular re-oxygenation. Assuming a Newtonian fluid and laminar fully developed flow, blood pressure and flow can generally be described by Poiseuille's Law,

$$\Delta P = \frac{8\mu LQ}{\pi R^4}$$

where changes in pressure, P , are directly proportional to blood viscosity, μ , vessel length, L , and blood flow, Q , and inversely proportional to the vessel radius, R , raised to the fourth power [2]. Exemplified in Poiseuille's equation, small changes in vessel radius

lead to large changes in pressure and/or flow. Arterioles preserve blood flow to tissues by modulating vessel diameters. A continuous layer of vascular smooth muscle cells surrounding the abluminal vessel wall regulates arteriolar dilation and constriction as dictated by local environmental cues. Tightly packed arterial smooth muscle cells are elongated perpendicular to flow, and circumferentially around vessels to optimally modulate blood pressure and flow. Endothelial cells lining arterioles elongate in the direction of flow in response to high shear stresses preserved by the arterial cascade [2]. Arterioles with decreasing diameters direct blood into capillaries, while venules with increasing diameters drain capillary networks into larger veins which return blood to the heart. Compared to arterial pressure, venous flow is sustained at low pressure by valves allowing flow in one direction. Large diameters compared to their analogous arterioles allow venules to conserve blood volume at low flows and pressures [2]. Accordingly, venous smooth muscle cells (SMCs) are not as tightly packed as arterial SMCs since they do not need to modulate vasotone as dynamically. Because flow through venules is low, endothelial cells lining venules are not elongated, but rather form a cobble-stone morphology [3].

Capillaries contain a thin layer of cells permitting the exchange of gases, solutes and other blood constituents between blood and tissue. As the site of oxygen and nutrient exchange for every tissue, capillaries are the most prevalent vessel type in the body. A basement membrane consisting of extracellular matrix supports capillary structure and sequesters biologically active molecules [2]. Located within the basement membrane, pericytes wrap around and elongate along capillaries, directly interacting with endothelial

cells by physical contact and by paracrine signaling. As suggested by their intimate relationship with endothelial cells, pericytes are essential for microvascular functions such as vascular remodeling, regulation of capillary blood flow and modulation of capillary permeability [4,5].

As indicated by the structural and functional heterogeneity across the microvascular hierarchy, proper vascular network architecture is fundamental for normal microvascular function, tissue oxygenation and even drug delivery [6]. Determining how microvascular networks develop and remodel is critical to understanding its function in normal tissue and its role in pathological scenarios. However, microvascular development and remodeling is a complex continuum of processes which persist from development through adulthood [7]. Microvascular networks dynamically respond to a plethora of environmental stimuli to suit local tissue demands and coordinate growth with multiple systems. Thus, harnessing the microvasculature for therapeutic purposes requires understanding its relationships with multiple systems across the microvascular hierarchy during remodeling processes.

1.2.2 Angiogenesis

The growth of new blood vessels from existing vasculature, termed angiogenesis, is a paramount remodeling process for normal development and healthy adulthood. During development, rapid angiogenesis creates the highly stereotyped and hierarchical vascular system lined by endothelial cells. Through adulthood, the vasculature remains fairly quiescent and endothelial cell proliferation is relatively low [8]. Normal angiogenesis in

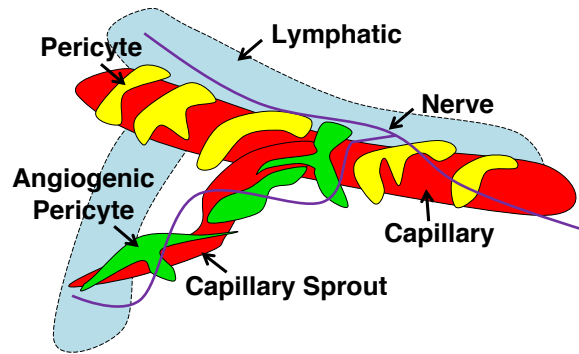


Figure 1: Multicellular and Multisystem Interactions during Angiogenesis. Angiogenesis is a complex process involving multiple cell types, such as endothelial cells and pericytes, and multiple systems, such as the nervous and lymphatic systems. Phenotypes of the same cells differ across intact networks during angiogenesis, further complicating the process.

the adult occurs during wound healing and endometrial formation after menstruation,

highlighting the vascular capability to revert to an angiogenic state. *Aberrant*

angiogenesis in adults is a common denominator for over 70 disease pathologies

including cancer, diabetic retinopathy, stroke and cardiovascular disease, making its

manipulation a central target for therapeutic advancement [9]. For example, excessive

angiogenesis fuels diseased tissue and can lead to progression of the disease, as is the

case for tumor growth. Deficient vessel growth leads to inadequate circulation and death

of healthy tissue. The line between excessive and deficient is described as a balance of

effective pro- and anti- angiogenic factors which, when in check, maintain vascular

homeostasis. While high concentrations of pro-angiogenic factors such as Vascular

Endothelial Growth Factor (VEGF) and Fibroblast Growth Factor (FGF) are associated

with aggressive angiogenesis, anti-angiogenic factors may be concurrently down-

regulated, further tipping the pathology toward an angiogenic phenotype [8,10]. Current

therapies focus on reversing the angiogenic phenotype or restoring circulation by

stimulating angiogenesis. However, angiogenesis is a complex process involving multiple

cell types, such as endothelial cells and pericytes, which often vary in phenotype across

intact networks during angiogenesis [11]. In addition, multiple systems, such as the nervous and lymphatic systems, interact with the vasculature during angiogenesis (Figure 1) [4,7,12]. This thesis focuses on the anatomical and phenotypic relationships between the nervous system and microvasculature which dictate functional interactions during angiogenesis. Despite significant advances in microvascular research, therapeutic efficacy in angiogenic related diseases remains limited. Future success depends on understanding these complex cellular and molecular interactions to develop multifaceted therapies and synergistic targeting strategies.

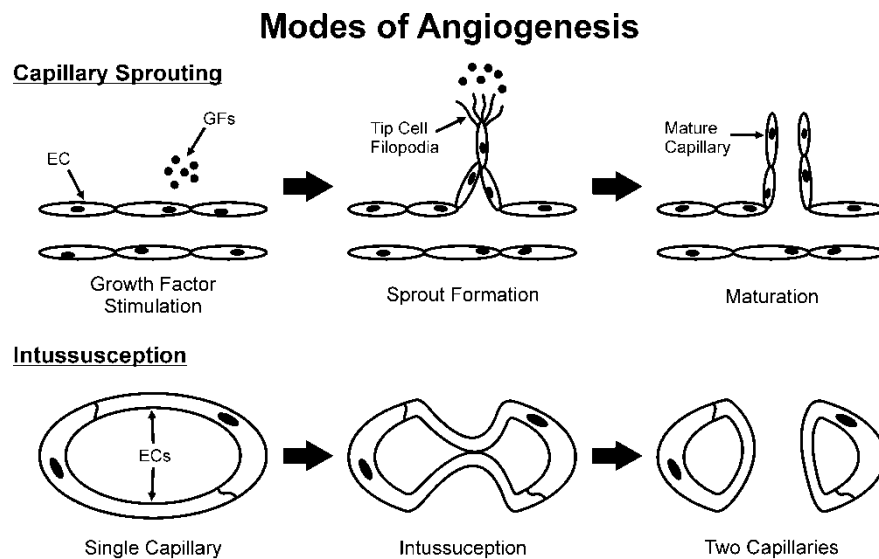


Figure 2: Modes of Angiogenesis. Angiogenesis by capillary sprouting involves a tip cell migration toward a growth factor stimulus, followed by stalk cell proliferation and extension. Intussusception occurs when a single capillary splits into two adjacent capillaries. Image provided by Richard Sweat.

Angiogenesis is traditionally characterized by two modes: sprouting and splitting, also called intussusception [7]. In sprouting angiogenesis, an endothelial cell, called the tip cell, responds to a growth factor gradient by orienting itself in the direction of the gradient (Figure 2) [13]. Various cells within the tissue microenvironment dynamically produce pro-angiogenic factors when new blood vessels are necessary. For example,

during development, nerves can secrete VEGF to instruct vascular patterning [14]. While multiple factors are documented angiogenic stimuli, VEGF is considered the most potent. Subsequent degradation of the basement membrane encapsulating the sprout location allows the tip cell to migrate up the gradient, and may release growth factors from the extracellular matrix (ECM). Followed by the tip cell are proliferating endothelial stalk cells which also migrate and then form the lumen of the new capillary [15]. The sprouting capillary joins with existing vasculature to form a functional capillary. Pericytes physically interact with endothelial tip and stalk cells, wrap around capillaries and capillary sprouts, and in some cases lead capillary sprouts. They play functional roles during angiogenesis including deposition and degradation of basement membrane, growth factor presentation to endothelial cells, stabilization of newly connected capillaries, and regulation of endothelial cell quiescence [16].

1.3 Microvascular and Neural Links

1.3.1 Anatomical

The vascular and neural systems are intimately linked by their functional interdependence. Neurons require oxygen and nutrients delivered by blood vessels, while vasotone is regulated by sympathetic innervation [17]. Not unexpectedly, vascular and neural networks exhibit similar anatomical patterns (Figure 3). They are both highly branched, hierarchical structures with efferent and afferent pathways. During development, the vascular and neural systems grow along concomitant routes, and establish shared anatomical pathways which remain throughout adulthood. Furthermore, these pathways are stereotyped, meaning conserved within species [12,18]. Ongoing research focuses on understanding the patterning mechanisms which result in similar vascular and neural structures.

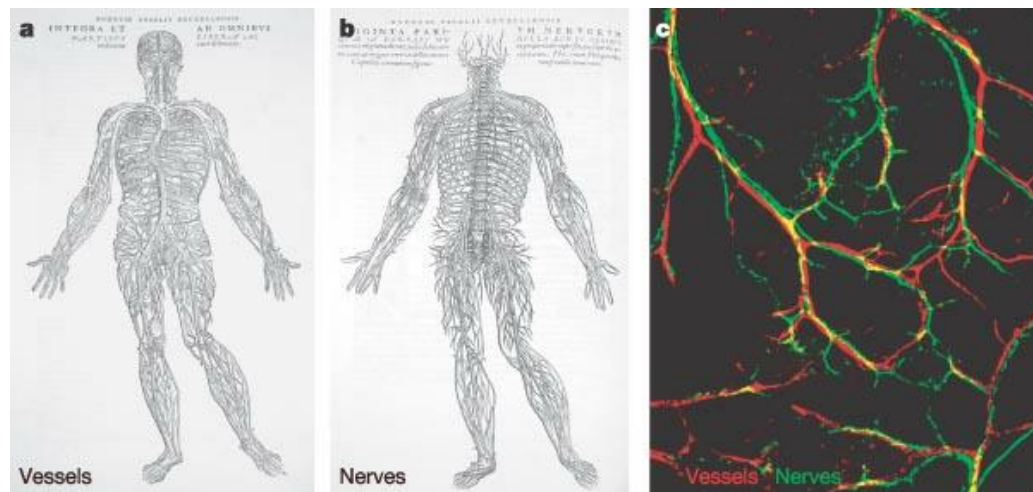


Figure 3: Neurovascular Alignment. Vessels and nerves follow similar anatomical pathways on the (a and b) macro- and (c) micro-scales. Adapted from Carmeliet & Tessier-Lavigne [12].

1.3.2 Growth Mechanisms

Emerging evidence suggests that the vascular and nervous systems are intimately linked because the vascular system co-opted growth mechanisms and cues from the nervous system [12,19-21]. This is supported by recent work highlighting the common molecular signals and cell dynamics involved in angiogenesis, and its neural analog, neurogenesis [19]. Overlap signaling molecules such as ephrins and their Eph receptors, Slits and their Robo receptors, semaphorins and their plexin and/or neuropilin receptors, and netrins and their DCC and Unc5 receptors direct the growth of both systems starting during development and demonstrate their intersecting phenotypes [12,18,22]. Leading vascular and neural cells also display similar morphologies. Tip cells, leading capillary sprouts, and axon growth cones, leading neural growth, are highly migratory and extend filipodia to explore potential routes for guidance signals [12,19]. Furthermore, both guiding cell types often follow gradients of growth factors – VEGF and Nerve Growth Factor (NGF), respectively [12]. The hierarchical branching structures and pathways that the vascular and neural systems share are the result of these neural-vascular overlaps (Figure 3). While many of these patterns established during development, the neurovascular relationship persists throughout adulthood while normal microvascular remodeling continues to reshape the microcirculation in non-stereotyped pathways. The extent of neurovascular coordination along adult angiogenic microvascular networks and how one network influences the growth pattern of the other remains under-investigated.

Neural networks are capable of influencing microvascular patterning and, conversely, microvascular networks can direct neural growth. During development in the avian

forelimb, neurovascular alignment arises as major vessels and nerves independently follow stereotyped pathways in cases of either vascular or neural lead growth [23-25]. Neuronal precursors pre-existing in the adult brain are able to induce angiogenesis and endothelial cell tube formation [26]. During development, neurons can also secrete VEGF to influence capillary sprouting and arterial differentiation [27,28]. In the adult retina, pre-existing glial cells were observed to guide capillary sprout formation [13]. However, whether nerve-derived factors also regulate angiogenesis in other adult tissues remains under-investigated. In contrast, angiogenesis has been shown to precede neurovascular alignment. For example, the initial capillary plexus in embryonic mouse limb skin is established before neural in-growth [14,28]. In adult wound healing and skin graft models, innervation follows vascular patterns established during tissue vascularization [29,30]. While these studies have provided valuable information regarding the potential patterning relationships between the two systems, insight into their interdependence during the angiogenic process can be gained by examining the extent of neurovascular alignment across a remodeling adult microvascular network. All together links between the vascular and neural systems are just beginning to be characterized and offer an exciting new perspective on the study of adult microvascular remodeling.

1.4 Pericytes in the Microcirculation

1.4.1 Function in the Microvasculature

Vascular pericytes are critical players in the microcirculation. Also called Rouget cells or mural cells, they are defined morphologically as cells within the basement membrane that elongate along the long axis of capillaries, and wrap around endothelial cells with shorter processes [4,31]. Direct interdigitations protrude from pericytes into endothelial cells at their interface, and endothelial processes reciprocate [32]. Pericyte coverage is heterogeneous among organs depending on the needs of the local tissue environment. In the brain, for example, a high density of pericytes tightly regulates the blood-brain barrier as a selectively permeable fortification which prevents fluctuations in the central nervous system's sensitive environment. Pericyte coverage in skeletal muscle, however, may be as low as 1 pericyte for every 100 endothelial cells [5].

Pericytes are functionally associated with blood vessel diameter regulation, vessel permeability, endothelial cell proliferation and angiogenesis [16,31]. Recent evidence shows that pericytes regulate capillary diameter by contraction in response to neurotransmitter stimulation [33], implicating pericytes as highly localized modulators of blood flow. Lack of pericyte recruitment leads to endothelial hyperplasia and increased vascular permeability [34,35], associating pericytes with vessel stability and maturation. Angiopoietin 1 (Ang1), a pericyte derived paracrine signal for the endothelial receptor Tie2, is essential in regulating endothelial quiescence and vessel maturation. Loss of the Ang1-Tie2 signaling loop leads to abnormal vascular patterns and impaired pericyte recruitment [36]. In pericyte deficient retinas, recombinant Ang1 rescues morphological

vascular defects, eliminated edema, and increased pericyte coverage, demonstrating its essential role in vascular stabilization [37]. Work on pericyte physiology has established that, in addition to Ang1/Tie2 signaling, the pericyte-endothelial cell communication is governed by TGF- β and PDGF-B/PDGFR- β interactions [38]. However, the full scope of intercellular signaling between pericytes and endothelial cells remains unknown.

1.4.2 Function during Angiogenesis

In addition to regulating vessel stabilization, pericytes play a central role in angiogenesis. During angiogenesis, pericytes have been implicated in paracrine signaling with endothelial cells, and extracellular matrix assembly [4]. They have also been shown to lead sprouting endothelial cells and bridge the gaps between two sprouting segments in some cases [39,40]. As such, pericytes have emerged as a cellular target to manipulate angiogenesis [41,42].

Endothelial cells of newly forming vessels recruit pericytes by secreting platelet-derived growth factor B (PDGF-B), to which pericytes migrate [43,44]. Manipulating pericyte investment by altering recruitment to the endothelium can cause lethal microvascular dysfunction, affect vascular patterning during development, and affect the formation of new vessels during physiological and pathological angiogenesis [4,45]. As previously described, this can be attributed to pericyte regulation of endothelial cell proliferation. Recent work has also identified pericytes as important players in regulating basement membrane organization. During developmental vascular assembly, pericytes catalyze deposition of basement membrane proteins including collagen IV, laminin and

fibronectin. Furthermore, pericyte-endothelial cell interactions induce changes in expression of extracellular matrix-binding integrins by both cell types, which are necessary for investment in newly formed matrix [46]. Once vascular tubes are assembled, pericyte-derived tissue inhibitor of metalloproteinase-3 (TIMP-3) prevents proteolysis of matrix proteins [47]. While it is clear that pericyte-endothelial cell interactions play a crucial role in establishing and maintaining a normal microcirculation, questions about pericyte mechanisms, especially during angiogenesis in the adult remain. Determining phenotypic differences between pericytes on angiogenic vessels and mature vessels may provide insights to the varying functions of pericytes across the microvasculature.

1.4.3 Heterogeneous Phenotypes

Pericyte heterogeneity within the hierarchy of microvascular networks, and across tissue-types has been a major barrier to further elucidating pericyte mechanisms. While true pericytes reside on capillaries and capillary sprouts, perivascular cells which resemble smooth muscle cells and pericytes reside where capillaries transition from arterioles or to venules [48]. Common pericyte markers include smooth muscle α -actin (SM α A), desmin, vimentin and PDGFR- β , but their expression is not specific to pericytes [4]. Additionally, their expression is distributed heterogeneously along the hierarchy of a network, and their overlap varies among pericytes [48]. The next critical step to advancing pro- or anti- angiogenic therapies aimed at pericytes will require the ability to identify specific populations of pericytes and their related dynamics.

Similarities between pericytes and smooth muscle cells blur distinctions between the two cell types. Pericytes differentiate into smooth muscle cells as vessels mature. TGF- β signaling has been shown to induce SM α A expression in pericytes and reduce their proliferation, indicating its role in mediating pericyte differentiation [49]. Pericytes have also shown the capacity to differentiate into osteogenic [50], macrophage/dendritic [51] and neural phenotypes [52] suggesting their potential as multipotent stem cells.

1.4.4 Neural Phenotypes

In addition to overlapping signaling molecules, vascular and neural cells share other phenotypic similarities. In recent years Neuron-glial antigen 2 (NG2), a marker of glial and neural progenitor cells in the central nervous system, has been identified as a marker of vascular pericytes [53]. NG2 identifies perivascular cells along arteries (Figure 4), capillaries and capillary sprouts, and is transiently up-regulated along remodeling venules during angiogenesis [11,54]. The identification of NG2 led to the establishment of its functional role in mediating endothelial cell dynamics associated with capillary sprouting [55], and highlights the overlap between signaling molecules present in the vascular and neural systems. The common use of NG2 as a pericyte marker and its characterization raises the question of whether other neural phenotypic markers identify pericytes during angiogenesis. The transient expression of NG2 during angiogenesis also stresses the need to understand different functions of pericytes on remodeling vasculature versus those on mature vessels. Similar to NG2, class III β -tubulin is considered a marker of neural progenitor cells in the CNS and peripheral nerves in the adult [56,57].

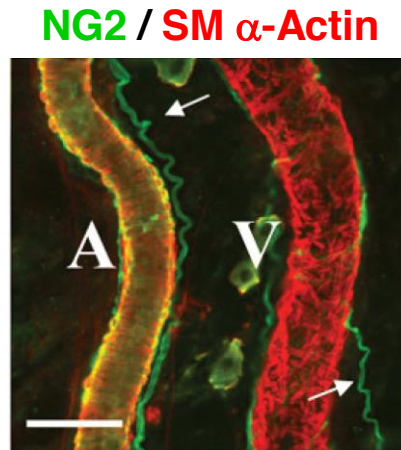


Figure 4: NG2 Expression by Pericytes. NG2 identifies nerves (arrows) and perivascular cells along arteries (A), capillaries and capillary sprouts in unstimulated tissue. Scale bar = 50 μ m. Image adapted from Murfee et al., 2005 [54].

Class III β -tubulin is one of seven β -tubulin isotypes which form α/β -tubulin heterodimers with six β -tubulin isotypes during the assembly of microtubules [57]. In the central nervous system, III β -tubulin is an early neuron-specific cytoskeletal marker during development, and has been associated with neuronal differentiation and neurogenesis [58]. Additionally, it is a cytoskeletal component in peripheral nerves and has been linked to prolonged cell cycling, cell survival, and cell migration [59,60]. Although class III β -tubulin expression is almost entirely specific to the nervous system in normal tissues, its expression in non-neuronal cancers correlates with resistance to tubulin-binding agents, high metastatic potential and malignancy [57,59,61,62]. Proteins associated with III β -tubulin expression are also involved in cellular responses to oxidative stress and glucose deprivation [63]. Still, specific functions of class III β -tubulin are unclear and future studies will be required to determine its mechanistic role during angiogenesis.

1.5 Models for Studying Angiogenesis

1.5.1 *In Vitro*

In vivo use of growth factors is associated with potential systemic effects, unknown delivery efficacy and a lack of local environmental control. Probing specific cellular and molecular interactions by functional inhibition or interference also correlate with the

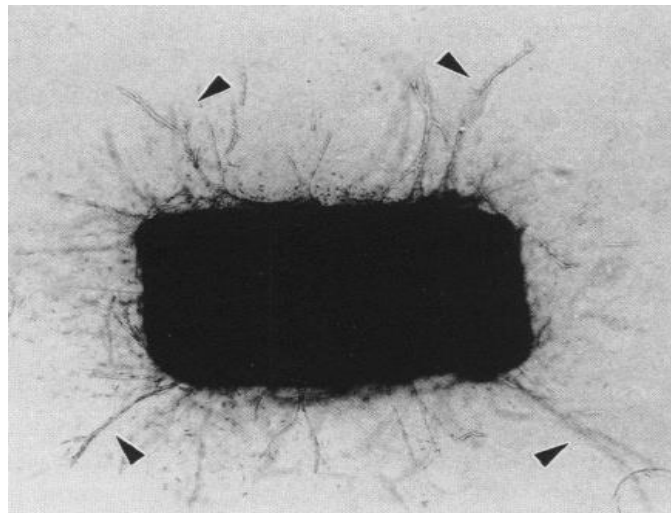


Figure 5: The Aortic Ring Assay. Endothelial cell sprouting (arrow heads) in the aortic ring assay is quantifiable, but does not occur from physiological microvascular networks. Image adapted from Villaschi & Nicosia, 1993 [71].

same problems. Although *in vitro* techniques lose physiological relevance, they provide a controlled environment to examine specific mechanisms [64]. Common *in vitro* assays for angiogenesis involve two-dimensional culture on tissue culture plastic or a matrix, or three-dimensional culture of cells within a matrix, such as Matrigel. Such techniques have been essential for characterizing isolated cell functions such as proliferation and migration, and the molecular players which regulate those processes [65]. Co-culture systems incorporate more than one cell type, and are used to investigate cell-cell interaction, such as those between pericytes and endothelial cells [66]. While contributions of *in vitro* experimentation are incontrovertible, their results must be

confirmed in models which represent their physiological environment to validate their significance. *Ex vivo* models provide an option to investigate cellular functions within a tissue space *in vitro*, providing a controlled setting which resembles the *in vivo* microenvironment [67]. The aortic ring assay is a common *ex vivo* model for studying angiogenesis. A slice of rat or mouse aorta is stripped of its adventitia and embedded within a collagen gel [68]. Endothelial cells sprout radially from the explanted tissue and recruit pericytes and smooth muscle cells (Figure 5) [69-71]. Sprouting is quantifiable using phase microscopy and immunohistochemical labeling methods, and can be manipulated with pro- and anti-angiogenic factors [68]. Limitations of this model include difficulties quantifying the three-dimensional growth that occurs, and the fact that angiogenesis occurs from capillaries and venules, not from aortas [64]. Thus, there is a clear need for an assay which provides quantifiable angiogenesis from *intact* microvascular networks in a controllable environment.

1.5.2 The Adult Rat Mesentery as an *In Vivo* Model of Angiogenesis

In vivo and *in vitro* assays each present advantages and disadvantages to studying angiogenesis as with most biological studies. *In vivo* models represent angiogenesis in normal and pathological scenarios within real vascular networks, but complicate analysis of specific mechanisms. The adult rat mesentery is a model to study the interactions of multiple cell types involved in microvascular remodeling [11,40]. It allows two dimensional observations across the entire hierarchy of intact microvascular, neural and lymphatic networks down to the cellular and sub-cellular level at different time points during microvascular remodeling. Unstimulated tissues display nominal levels of

angiogenesis intrinsic to physiological vascular network expansion within mesenteric windows. Inflammatory angiogenesis can be stimulated by exteriorization of the tissue or by intra peritoneal (i.p.) injection of a mast cell degranulator, compound 48/80 [72,73]. Compound 48/80 incites an inflammatory reaction in mesenteric windows by mast cell activation and histamine release. Although the exact triggering mechanisms are unclear, stimulation with compound 48/80 quickly causes a robust vascular response by mechanisms inherent to the angiogenic process resulting in microvascular remodeling [73,74]. Exposing the rat to chronic hypoxia stimulates a more physiological model of angiogenesis and is relevant to tissue ischemia scenarios [11,75]. I.p. injections of VEGF and bFGF, two potent angiogenic growth factors, stimulate angiogenesis allowing investigation of the angiogenic time course and dose-dependent responses, highlighting the model's potential to probe pro- and anti-angiogenic stimuli [76,77]. This model has also been used to characterize NG2 expression by perivascular cells per vessel type during angiogenesis [11,54]. Still, neither an *in vivo* nor *in vitro* model to probe multicellular and multisystem interactions during angiogenesis in intact microvascular networks within a controlled environment exists.

1.6 Specific Aims

Abnormal microvascular remodeling is associated with the progression of multiple disease pathologies including cancer, diabetic retinopathy and hypertension. Accordingly, the microvasculature has been a target for therapies that aim to treat such diseases. Success however, requires a better comprehension of microvascular remodeling mechanisms, including angiogenesis. Defined as the growth of new vessels from existing vessels, angiogenesis involves multiple vascular cell types such as endothelial cells and pericytes, and multiple systems including the lymphatic and nervous systems. In order to fully understand angiogenesis, we must probe the multi-cellular interactions among cells within the microvasculature and its relationships with lymphangiogenesis and neurogenesis. An emerging area of microvascular research focuses on the links between the vasculature and nervous system, stemming from evidence suggesting that the vascular system co-opted growth mechanisms and cues from the neural system. Anatomical similarities include hierarchical structures and pathways, while the two systems also share common molecular signals and protein expression. Identifying such system-level relationships and discerning their functional interplay is critical to comprehending abnormal microvascular remodeling, and engineering functionalized tissues. However, functional interactions and commonalities between the microvasculature and nervous system during angiogenesis remain under-investigated.

The overall objectives of this work are to: 1) identify links between the microvasculature and nervous system during angiogenesis in the adult and 2) establish a model to probe specific cellular and molecular interactions within intact microvascular networks and

across systems in a controlled environment. The specific aims to complete the objectives are as follows:

Aim 1: Determine the spatiotemporal relationship between angiogenesis and neurovascular alignment.

Angiogenesis was stimulated in adult male Wistar rats by i.p. injection of compound 48/80, a mast cell degranulator. Mesentery tissues were immunolabeled for class III β -tubulin (neural marker) and PECAM (endothelial marker) in unstimulated tissues and 2, 10 and 30 days after stimulation. Capillary sprout and vessel densities were quantified as angiogenic indices. The density of vessels aligned with nerves (neurovascular alignment) was quantified to determine the spatial and temporal relationship between angiogenesis and neurogenesis.

Aim 2: Determine whether class III β -tubulin is a functional marker of perivascular cells during angiogenesis.

Aim 2a: Determine the perivascular cell expression pattern of class III β -tubulin (a neural marker) during angiogenesis.

Angiogenesis was stimulated in adult male Wistar rats by i.p. injection of compound 48/80. Mesentery tissues immunolabeled for class III β -tubulin and PECAM were evaluated 0, 2, 10 and 30 days after stimulation. Capillary sprout and vessel density was quantified as angiogenic indices. The density of vessels expressing class III β -tubulin at each time point was quantified per vessel type to determine the distribution of perivascular cells expressing a neural phenotype over the time course of angiogenesis.

Aim 2b: Determine the functional importance of class III β -tubulin during proliferation and migration in human vascular pericytes.

Class III β -tubulin function was examined in human brain vascular pericytes (hBVPCs) *in vitro*. hBVPCs were treated with siRNA to inhibit class III β -tubulin. Proliferation was assessed by analyzing the percentage of Ki67 positive nuclei in normal versus protein-inhibited cells. Migration was assessed 6 hours after a scratch wound on confluent monolayers of hBVPCs.

Aim 3: Develop an *in vitro* culture model using the adult rat mesentery to investigate multicellular and multisystem interactions during angiogenesis within intact microvascular networks.

Mesentery tissues were cultured in serum free media or serum free media supplemented with bFGF, VEGF and/or NG2 antibodies for 3 days. Tissues were immunolabeled for PECAM and NG2. Capillary sprout and vessel density per vessel identity was quantified to show that angiogenesis occurs in culture, and that growth factors can stimulate angiogenesis. Tissues were treated with NG2 function blocking antibodies to determine whether cell-cell interactions can be probed in the system.

The proposed work will offer novel insights into the link between the vascular and nervous systems by characterizing the spatial and temporal relationship between angiogenesis and neurogenesis in the context of neurovascular alignment and establishing class III β -tubulin as a target to investigate perivascular cells during angiogenesis. Additionally, this work will establish the mesentery culture model as a novel platform to

investigate angiogenesis, and elucidate the functional importance of class III β -tubulin expression by pericytes during angiogenesis. **The research is significant because it expands our knowledge of angiogenesis and may be used to develop novel therapies aimed at manipulating angiogenesis.**

CHAPTER 2: METHODS AND MATERIALS

2.1 Spatiotemporal Relationship between Angiogenesis and Neurovascular

Alignment

2.1.1 Mast Cell Degranulation Model

All experiments were performed in accordance with the guidelines of the Tulane University Care and Use Committee. Single 2 ml doses of compound 48/80 were injected i.p. over the time course of 3 days (twice a day and once on the final day) in increasing concentrations (200, 400, 600, 800 and 1000 $\mu\text{g/ml}$ in saline) into 350-450 g adult male Wistar rats, according to a previously established protocol [11]. Mesenteric windows were harvested and processed for immunohistochemistry according to the following experimental groups: Unstimulated (n = 4 animals), 2 days post-compound 48/80 stimulation (n = 4 animals), 10 days post-stimulation (n = 4 animals), and 30 days post-stimulation (n = 4 animals). A mesenteric window is defined as the thin translucent membrane in between the artery/vein pairs feeding the small intestine. Three end time points post 48/80 stimulus were included in the study to capture the initial time course of network growth. From each of the four animals per group, three randomly selected networks from randomly selected tissues were analyzed (n=12 tissues per time point). This particular model was selected because it produces a robust angiogenic response over the hierarchy of mesenteric microvascular networks within a relatively short time period.

2.1.2 Mesentery Exteriorization Model

All experiments were performed in accordance with the guidelines of the Tulane University Care and Use Committee. Similar to a previously established protocol [11], adult male Wistar rats (350-450 g) were anesthetized with i.m. injections of ketamine (80 mg/kg bw) and xylazine (8 mg/kg bw). Using sterile surgery technique, 8 mesenteric tissue windows, identified as the thin translucent connective tissues attached to the ileum, were gently removed from the abdominal cavity and placed on a specially designed sterile plastic stage. The mesentery region was then left exposed for 20 minutes. Over the time course of the 20-minute exposure, the tissue was superfused with saline solution. The two centrally located mesenteric windows were marked with 7-0 silk sutures. At the end of the 20-minute exposure duration the tissue was returned to the abdominal cavity and the incised muscle and peritoneal layers were sutured. After 3 days, rats were anesthetized again and euthanized via an intra-cardiac injection of beuthanasia. The previously exposed mesenteric windows were harvested and immunolabeled.

2.1.3 Chronic Hypoxia Model

All experiments were performed in accordance with the guidelines of the Tulane University Animal Care and Use Committee. Similar to a previously established protocol [11], adult male Wistar rats (350-450 g) were placed into a plexiglass hypoxia chamber (BioSpherix) while still in their respective cages. The chamber was purged with nitrogen gas to reduce oxygen levels to 10% volume of the chamber for 3 days. During the chronic hypoxia exposure, the oxygen levels inside the plexiglass chamber were monitored and maintained at $10 \pm 0.1\%$. Both carbon dioxide and moisture were monitored and

maintained at appropriate levels. The animals were checked visually through the transparent chamber twice daily to ensure that they were free of pain and distress, and that they maintained a healthy weight. The temperature and humidity inside the hypoxia chamber were also monitored daily to ensure acceptable conditions.

2.1.4 Immunohistochemistry

Tissues were fixed in methanol at -20 °C for 30 minutes, and then labeled with antibodies against PECAM (CD31) and class III β -tubulin, or class III β -tubulin and tyrosine hydroxylase (TH).

PECAM + class III β -tubulin: 1) 36 hour incubation at 4°C with 1:200 mouse monoclonal class III β -tubulin antibody (2G10, Abcam, Cambridge, MA); 2) 36 hour incubation at 4°C with 1:100 goat anti-mouse CY2-conjugated secondary antibody (Jackson ImmunoResearch Laboratories, West Grove, PA) and 5% normal goat serum (Jackson ImmunoResearch Laboratories, West Grove, PA), diluted in antibody buffer; 3) 1 hour incubation at room temperature with 5% normal mouse serum (Jackson ImmunoResearch Laboratories, West Grove, PA); 4) 1 hour incubation at room temperature with 1:200 mouse monoclonal biotinylated CD31 antibody (BD Pharmingen, San Diego, CA); 5) 1 hour incubation with CY3-conjugated Streptavidin secondary antibody buffer (Jackson ImmunoResearch Laboratories, West Grove, PA).

Class III β -tubulin + TH: 1) 36 hour incubation at 4°C with 1:200 rabbit polyclonal tyrosine hydroxylase antibody, and 1:200 mouse monoclonal class III β -Tubulin antibody, diluted in antibody buffer (0.1% saponin in PBS + 2% BSA); 2) 36 hour incubation at 4°C with 1:100 goat anti-rabbit CY2-conjugated antibody and 1:100 goat

anti-mouse CY3-conjugated secondary antibody (Jackson ImmunoResearch Laboratories), diluted in antibody buffer.

2.1.5 Imaging

Five-by-five image areas of the networks were captured using a 10x objective (Dry; NA = 0.3) on an inverted microscope (Olympus IX70) coupled with a PixelFly camera.

Higher magnification images (Figures 6, 7, 9 and 12) were acquired using a 20x (Oil; NA = .8) or 60x objective (Oil; NA = 1.4) and an inverted microscope (Olympus IX70) coupled with a Photometrics CoolSNAP EZ camera.

2.1.5 Quantification of Angiogenesis and Neurovascular Alignment

Vascular densities and neurovascular alignment was quantified per network (n=4 rats; 12 networks). A network was defined as having a feeding arteriole, draining venule and multiple branches. The number of vessel segments per image for arterioles ($> 20\mu\text{m}$), pre-capillary arterioles (10-20 μm), capillaries, post-capillary venules (10-20 μm), venules ($> 20\mu\text{m}$) and capillary sprouts were counted on every third image using the Java-based NIH image processing software ImageJ version 1.43u. Vessel types were identified by endothelial cell morphology, vessel diameter and location within the network. Blood vessels and nerves were considered aligned when they were within 10 μm of each other for at least 50 μm . The number of aligned vessel segments per vessel category was counted at each time point.

2.1.6 Statistical Analysis

Network remodeling and neurovascular alignment metrics were compared across the time course of angiogenesis after compound 48/80 stimulation using a one-way ANOVA followed by Tukey's pairwise comparison test (SigmaStat). Statistical significance was accepted for $p < 0.05$. Values are presented as mean \pm standard error of the mean.

2.2 Class III β -Tubulin as a Functional Marker of Perivascular Cells during Angiogenesis

2.2.1 Stimulation of Angiogenesis

All experiments were performed in accordance with the guidelines of the Tulane University Care and Use Committee. Similar to a previously established protocol [11], single 2 ml doses of compound 48/80 (200, 400, 600, 800 and 1000 μ g/ml in saline) were injected i.p. over the time course of 3 days (twice a day and once on the final day) in increasing concentrations into 350-450 g adult male Wistar rats (n=4 per time point). Tissues were harvested and processed for immunohistochemistry according to the following experimental groups: Unstimulated (n = 4 animals), 2 days post-compound 48/80 stimulation (n = 4 animals), 10 days post-stimulation (n = 4 animals), and 30 days post-stimulation (n = 4 animals). From each of the four animals per group, networks from two randomly selected tissues were analyzed (n=8 tissues per group). Three end time points post 48/80 stimulus were included in the study to capture the time course of capillary sprouting. This particular model was selected because it produces a robust angiogenic response over the hierarchy of mesenteric microvascular networks within a relatively short time period.

2.2.2 Alternative Models of Angiogenesis

All experiments were performed in accordance with the guidelines of the Tulane University Care and Use Committee. For chronic hypoxia stimulation of angiogenesis (See Section 2.1.3 Chronic Hypoxia Model; Figure 16B), animals were placed in a chamber and maintained at 10% oxygen for 3 days. The temperature, humidity and

carbon dioxide levels were monitored and maintained at normal levels. The mesentery exteriorization model entails exposing 8 mesenteric tissues outside the peritoneal cavity for 20 minutes (See Section 2.1.2 Mesentery Exteriorization Model; Figure 16A). Three days post exteriorization, tissues were harvested. Both models have been previously documented as angiogenic stimuli [11]. Tissues were immunolabeled for PECAM and class III β -tubulin.

2.2.3 Tissue Immunohistochemistry

Tissues were fixed in methanol at -20 °C for half an hour, and then labeled with antibodies against PECAM (CD31) and class III β -tubulin, or class III β -tubulin and NG2.

PECAM + Class III β -tubulin: 1) 36 hour incubation at 4°C with 1:200 mouse monoclonal class III β -tubulin antibody (2G10, Abcam, Cambridge, MA); 2) 36 hour incubation at 4°C with 1:100 goat anti-mouse CY2-conjugated secondary antibody (Jackson ImmunoResearch Laboratories, West Grove, PA) and 5% normal goat serum (Jackson ImmunoResearch Laboratories, West Grove, PA), diluted in antibody buffer; 3) 1 hour incubation at room temperature with 5% normal mouse serum (Jackson ImmunoResearch Laboratories, West Grove, PA);. 4) 1 hour incubation at room temperature with 1:40 mouse monoclonal biotinylated CD31 antibody (BD Pharmigen, San Diego, CA) ; 5) 1 hour incubation with CY3-conjugated Streptavidin secondary antibody buffer (Jackson ImmunoResearch Laboratories, West Grove, PA).

Class III β -tubulin + NG2: 1) 36 hour incubation at 4°C with 1:200 rabbit polyclonal NG2 antibody (Millipore/Chemicon, Billerica, MA), and 1:200 mouse monoclonal class

III β -Tubulin antibody; 2) 36 hour incubation at 4°C with 1:100 goat anti-rabbit CY2-conjugated antibody, 1:100 goat anti-mouse CY3-conjugated secondary antibody (Jackson ImmunoResearch Laboratories, West Grove, PA) and 5% normal goat serum. All antibodies were diluted in antibody buffer (0.1% Saponin in PBS + 2% BSA).

2.2.4 Tissue Imaging

Immunolabeled tissues were imaged on an inverted microscope (Olympus IX70) coupled with a PixelFly camera using 10x (Dry; NA = 0.3), and 20x (Oil; NA = .8) objectives, an inverted microscope (Leica DM IRE2) with a Leica SP2 AOB confocal microscopy system using 63x (Oil; NA = 1.4) objective, or an upright microscope (Nikon 90i) with a Nikon C1 confocal microscopy system using 4x (Dry; NA = 0.1), 20x (Dry; NA = 0.75) and 60x (Oil; NA = 1.4) objectives.

2.2.5 Quantification of Angiogenesis and Perivascular Cell Expression of Class III β -Tubulin

For unstimulated and each time point post 48/80 stimulation (day 2, day 10 and day 30), vascular densities and class III β -tubulin positive pericyte coverage per vessel type were quantified for 8 randomly selected tissues (2 tissues from each rat per experimental group). In each tissue, a microvascular network was analyzed. A network was defined as having a feeding arteriole, draining venule and multiple branches. Five-by-five image areas of the networks were captured using a 10x objective (Dry; NA = 0.3) on an inverted microscope (Olympus IX70) coupled with a PixelFly camera. The number of vessel segments per image for arterioles, capillaries, venules and capillary sprouts were counted

on every third image using the Java-based NIH image processing software ImageJ version 1.43u. Arterioles, capillaries, venules and capillary sprouts were identified by endothelial cell morphology, vessel diameter and location within the network. Vessel segments were considered to have class III β -tubulin positive cell coverage if at least one class III β -tubulin positive perivascular cell was observed to be present.

2.2.6 Statistical Analysis

The network remodeling and class III β -tubulin cell labeling metrics were compared across the time course of angiogenesis for the 48/80 mast cell degranulation model using a one-way ANOVA followed by a Student-Newman-Keuls pairwise comparison test (SigmaStat). Statistical significance was accepted for $p < 0.05$. Values are presented as means \pm standard error of the means.

2.2.7 Cell Culture

Human brain vascular pericytes (HBVP, 1200) were obtained from ScienCell (Carlsbad, CA) and maintained in Pericyte Medium (PM, 1201). Pericyte Medium contained 2% fetal bovine serum, 1% pericyte growth supplements and 1% 100x penicillin/streptomycin.

2.2.8 Inhibition of Class III β -Tubulin by siRNA

HBVPs were grown in plastic tissue culture flasks. Once confluent, cells were lifted using Trypsin/EDTA solution and neutralized using Trypsin Neutralizing Solution (ScienCell; Carlsbad, CA). Serum-free media, 30nM RNAiMAX (Invitrogen) and 30nM

siRNA were mixed in each culture well. Upon re-plating cells in 12-well tissue culture dishes, cells were transfected with class III β -tubulin siGENOME SMARTpool siRNA from Dharmacon/Thermo Scientific for 24 hours. SMARTpool siRNA reagents are a group of 4 siRNA oligos which target different parts of the class III β -tubulin gene to suppress expression. Suppression of class III β -tubulin expression was confirmed by immunohistochemistry after 72 hours.

2.2.9 Proliferation Assay

After 24 hours of transfection, HBVPs treated with no siRNA, control pool siRNA or class III β -tubulin siRNA were allowed to proliferate for 72 hours. HBVPs were fixed with methanol at -20°C and immunolabeled for Ki67, class III β -tubulin and nucleic acid. The percentage of Ki67 positive nuclei was quantified as an indicator of proliferating cells.

2.2.10 Migration Assay

After 24 hours of transfection, HBVPs treated with no siRNA, control pool siRNA or class III β -tubulin siRNA were grown to confluent monolayers for 48 hours. At 72 hours (24 hour transfection + 48 hours for gene suppression to manifest), each monolayer was scratched and imaged. Three groups were also treated with media containing 10nM paclitaxel, a tubulin binding drug, at the initiation of the scratch wound. After 6 hours, scratches were again imaged. The change in scratch area was quantified in 8 wells for each group.

2.2.11 Cell Immunohistochemistry

Class III β -tubulin + Ki67: 1) 12 hour incubation at 4°C with 1:200 rabbit polyclonal Ki67 antibody (Abcam; Cambridge, MA), and 1:200 mouse monoclonal class III β -Tubulin antibody (Abcam; Cambridge, MA), and 5% normal goat serum; 2) 1 hour incubation at room temperature with 1:100 goat anti-rabbit CY3-conjugated antibody, 1:100 goat anti-mouse CY2-conjugated secondary antibody (Jackson ImmunoResearch Laboratories, West Grove, PA) and 5% normal goat serum. 3) 10 minute incubation at room temperature with DAPI nucleic acid stain (Invitrogen). All antibodies were diluted in antibody buffer (0.1% Saponin in PBS + 2% BSA). Between incubation steps, samples were washed three times in PBS or 0.1% Saponin in PBS.

2.2.12 Cell Imaging

Immunolabeled cells were imaged on an inverted microscope (Olympus IX70) coupled with a PixelFly camera using 4x (Dry; NA = 0.1) or 20x (Oil; NA = .8) objectives. All image parameters were kept identical while collecting images to allow correlation between fluorescent intensity and class III β -tubulin expression.

2.2.13 Statistical Analysis

Ki67 percentages and scratch wound closure percentages were compared using a one-way ANOVA followed by a Student-Newman-Keuls pairwise comparison test (SigmaStat). Statistical significance was accepted for $p < 0.05$. Values are presented as

means \pm standard error of the means in figures, and means \pm standard deviation in the text.

2.3 The Adult Rat Mesentery as a Model for Multicellular and Multisystem

Interactions during Angiogenesis

2.3.1 Tissue Culture Method

All animal experiments were approved by Tulane University's Institutional Animal and Care Use Committee. Prior to harvesting tissue, an aseptic surgical area was prepared and instruments were sterilized. MEM containing Earle's Salts and L-Glutamine (MEM, Invitrogen) and 1% PenStrep (Invitrogen), saline and PBS with CaCl_2 and MgCl_2 were heated to 37°C. Adult male Wistar rats (325 – 425g) were anesthetized via intramuscular injection with ketamine (80 mg/kg b.w.), xylazine (8 mg/kg b.w.), and atropine (0.08 mg/kg b.w.). After 5 mins, the effect of anesthesia was confirmed and the rat's abdominal hair was shaved and removed. The abdominal skin was sterilized with alternating 70% isopropyl alcohol and iodine wipes. Using a scalpel blade, a (0.75 inch) longitudinal incision was made along the skin, and then the linea alba 1 inch below the sternum. Using cotton tip applicators, the ileum was located as a reference point. Then, the mesentery was gently pulled through a sterile plastic stage, and laid out. Sterile saline at 37°C was continuously dripped onto the tissue to keep it hydrated. See Yang et al. for details on harvesting mesentery tissue and the plastic stage [78]. Once the mesentery was exposed, the rat was euthanized by intracardiac injection of 0.1 – 0.2 ml Beuthanasia (Schering-Plough Animal Health).

Mesentery tissues were aseptically harvested from the gut using microscissors and forceps. A mesenteric window was defined as the thin, translucent connective tissue found between artery/vein pairs feeding the small intestine. Minimal fat that bordered

each window was cut with each tissue to reduce fat content in the cultures, and to avoid puncturing large blood vessels or the bowel. Tissues were immediately rinsed in sterile PBS with CaCl_2 and MgCl_2 at 37°C , and immersed in sterile MEM containing 1% PenStrep. After tissues were harvested, they were transported to a sterile culture hood. Tissues were rinsed in sterile PBS and MEM again at 37°C , then transplanted into 12-well culture plates (Invitrogen) containing media for each experimental group. One tissue was placed in each well with 2 ml of media for 3 or 7 days under standard cell culture conditions, and media was changed every 2 days.

2.3.2 Stimulation of Angiogenesis and NG2 Inhibition

To stimulate angiogenesis, media was supplemented with 60 ng/ml of recombinant human bFGF (Invitrogen) or 200 ng/ml of recombinant rat VEGF₁₆₄ (R & D Systems). NG2 function was blocked by supplementing media with 10 $\mu\text{g/ml}$ of rabbit polyclonal NG2 function-blocking antibody (Millipore/Chemicon). Rabbit IgG (Jackson ImmunoResearch Laboratories) at the same concentration as NG2 antibody (10 $\mu\text{g/ml}$) was added to growth factor supplemented media as an additional control group for non-specific rabbit-derived antibody binding. Each growth factor (GF) study included 4 experimental groups: 1) Control (MEM alone); 2) MEM + GF 3) MEM + GF + NG2 antibody 4) MEM + GF + Rabbit IgG. For both studies, 12 tissues from 4 rats were harvested and split evenly into the experimental groups (n=12 per group). As an immunohistochemical control for NG2 targeting, tissues cultured with VEGF + Rabbit IgG were incubated with GAR CY2-conjugated antibody alone.

2.3.3 Immunohistochemistry

For viability/cytotoxicity, tissues were incubated in Calcein AM and EthD-1 in PBS at 37°C for 10-15 minutes using the LIVE/DEAD Viability/Cytotoxicity Kit (Molecular Probes). Then they were rinsed in PBS and spread on slides for microscopy using forceps. For all other immunohistochemistry, tissues were spread on slides, fixed in methanol at -20°C for 30 minutes, and then labeled with antibodies against platelet endothelial cell adhesion molecule (PECAM; CD31) and Neuron-glia antigen 2 (NG2), smooth muscle α -actin (SM α A), lymphatic vessel endothelial hyaluronan receptor-1 (LYVE-1), class III β -tubulin or Bromodeoxyuridine (BrdU). All antibodies were diluted in antibody buffer solution (PBS + 0.1% Saponin + 2% BSA). Between antibody incubation periods, tissues were washed with cold PBS with 0.1% Saponin for ten minutes, three times.

PECAM + NG2: 1) 1 hour incubation at room temperature with 1:200 mouse monoclonal biotinylated CD31 antibody (CD31 antibody, BD Pharmingen) and 1:100 rabbit polyclonal NG2 antibody (Millipore/Chemicon, Billerica, MA) and 5% normal goat serum (NGS, Jackson ImmunoResearch Laboratories); 2) 1 hour incubation with 1:500 CY3-conjugated Streptavidin secondary (Strep-CY3) and 1:100 goat anti-rabbit CY2-conjugated antibody (GAR-CY2) with 5% NGS [11]. For NG2 functional studies, NG2 targeting was confirmed by labeling tissues with only the secondary antibody.

PECAM + SM α A: 1) 1 hour incubation at room temperature with 1:200 CD31 antibody
2) 1 hour incubation with CY2-conjugated Streptavidin secondary (Jackson

ImmunoResearch Laboratories) and 1:200 CY3 conjugated mouse monoclonal SM α A antibody (Sigma-Aldrich) [11].

PECAM + LYVE-1: 1) 1 hour incubation at room temperature with 1:200 CD31 antibody and 1:100 rabbit polyclonal LYVE-1 antibody (AngioBio) and 5% NGS; 2) 1 hour incubation with 1:500 Strep-CY3 and 1:100 GAR-CY2 with 5% NGS [79].

PECAM + Class III β -tubulin: 1) 36 hour incubation at 4°C with 1:200 mouse monoclonal class III β -tubulin antibody (2G10, Abcam) with 5% NGS; 2) 36 hour incubation at 4°C with 1:100 goat anti-mouse CY2-conjugated secondary antibody (GAR-CY2, Jackson ImmunoResearch Laboratories) and 5% NGS; 3) 1 hour incubation at room temperature with 5% NGS; 4) 1 hour incubation at room temperature with 1:200 CD31 antibody; 5) 1 hour incubation with 1:500 Strep-CY3 [80].

BrdU + PECAM: Prior to fixation, tissue was incubated in media with BrdU (Sigma-Aldrich) for 2 hours under standard culture conditions. After tissues were spread on slides and fixed in MeOH, they were incubated in 6 mol/L HCL for 1 hour to denature the DNA. Tissues were then washed in PBS + 0.1% Saponin, and incubated with antibodies against PECAM and BrdU: 1) 1 hour incubation at room temperature with 1:100 mouse monoclonal anti-BrdU (Dako) and 5% NGS; 2) 1 hour incubation at room temperature with 1:100 GAR-CY2 Fab fragments (Jackson ImmunoResearch Laboratories) and 5% NGS; 3) 1 hour incubation at room temperature with 1:200 CD31 antibody; 4) 1 hour incubation with 1:500 Strep-CY3 [81].

2.3.4 Imaging

Images were acquired using 4x (Dry; NA = 0.1), 10x (Dry; NA = 0.3), 20x (Oil; NA = 0.8 or Dry; NA = 0.75) and 60x (Oil; NA = 1.4) objectives on an inverted microscope (Olympus IX70) coupled with a Photometrics CoolSNAP EZ camera. Network images quantified for vascular data were captured using the 4x objective. Confocal microscopy of lymphatic/blood endothelial cell connections were captured with a 63x (Oil; NA = 1.4) objective on an inverted microscope coupled with a Zeiss LSM 510 confocal system. Twenty images were captured at 0.5 μm intervals (9.5 μm depth) with an optical thickness less than 0.7 μm . Lymphatic vessel filopodia images were acquired using a 60x (Oil; NA = 1.4) objective and the Olympus IX70-CoolSNAP microscope-camera combination. Images were captured in 0.5 μm intervals through an 8 μm depth, and processed through Nikon Extended Depth of Focus (EDF) software to generate all-in-focus images.

2.3.5 Quantification of NG2 Expression

Eight mesenteric tissues from 4 different rats were harvested and immediately labeled for PECAM/NG2, representing pre-culture expression of NG2. Eight mesenteric tissues from 4 different rats were harvested and cultured for 7 days in MEM + 1% PenStrep. Feeding and draining arterioles and venules were visually assessed as NG2 positive or negative in three tissues from each rat (n=12) at each time point. Capillary expression of NG2 was assessed in characteristic 4x network images from pre-cultured and 3 day cultured tissues.

2.3.6 Quantification of Angiogenesis

Endothelial sprouting and capillary density were quantified per tissue from 4x images of randomly selected networks in each tissue. For each tissue, up to five randomly selected areas were imaged to represent all microvascular networks. At least 1 network was imaged in each tissue. In the case that a tissue had only one network less than five fields of view in size, the entire network was imaged. A network was defined as having a feeding arteriole, draining venule and multiple branches. Data was collected from 4x images using the Java-based NIH ImageJ image processing software version 1.43u. The number of capillary sprouts was quantified per 3 groups: capillary sprouts originating from arterioles larger than 20 μm , capillary sprouts originating from venules larger than 20 μm , and capillary sprouts originating from capillaries. Capillary sprouts were defined as blind ended PECAM positive endothelial cell segments. Sprouting was quantified from arterioles and venules larger than 20 μm in order to demonstrate the ability to examine the locations of sprouting across the hierarchy of a network. Twenty microns was selected because, for this diameter threshold, arterial versus venous identities are clearly distinguishable. Arterioles versus paired venules exhibit smaller diameters and have more elongated cells [11,75,82]. Additionally, arterioles in this diameter range differentially label for NG2 compared to venules [54].

2.3.7 Quantification of Lymphatic/Blood Endothelial Cell Connections

Lymphatic/blood endothelial cell connections were quantified per overlapping lymphatic/blood vessel area. Direct connections between lymphatic and blood endothelial cells in rat mesenteric microvascular networks were previously characterized

by Robichaux et al [79]. Consistent with this previous study, lymphatic/blood endothelial cell connections in this study were identified based on 1) overlap of PECAM staining, 2) PECAM staining in the same focal plane and 3) a shared cellular or staining morphology. PECAM positive lymphatic vessel were distinguished from blood vessels by their larger diameter, more irregular diameter, decreased labeling intensity, and endothelial cell morphology [83]. Lymphatic/blood endothelial cell connections were identified based on continuous PECAM labeling and a shared cellular morphology [79]. Data was collected from the representative images from each tissue using the Java-based NIH ImageJ image processing software version 1.43u.

2.3.8 Statistical Analysis

Mann-Whitney rank sum tests were used to compare the percentage of NG2 positive arterioles and venules between pre- and post-culture groups. A student's t-test accounting for unequal variances was used to compare the percentage of NG2 positive capillaries between pre- and post-culture groups. Capillary sprouting metrics were compared across experimental groups using one way ANOVA followed by pairwise comparisons with the Student-Newman-Keuls method. Lymphatic/blood endothelial cell connection densities were compared between the growth factor stimulated groups and respective control groups using a student's t-test. For all tests, statistical significance was accepted when $p < 0.05$. Statistical tests were run on SigmaStat 3.5 software.

CHAPTER 3: RESULTS

3.1 Spatiotemporal Relationship between Angiogenesis and Neurovascular Alignment

3.1.1 Neurovascular Alignment across the Microvascular Hierarchy

Neurovascular alignment in unstimulated adult male rat mesenteric microvascular networks was observed along arterioles, venules, and capillaries (Figure 6). Along capillary sprouts, examples of nerve alignment were also observed (Figure 7). Nerves both led and lagged the endothelial tip cell. Alignment was most frequent in proximal regions of the network along feeding arterioles and draining venules (Figure 8A). After 10 days post 48/80 stimulation, networks displayed a dramatic increase in vessel density (Figure 8B), yet the increase in new vessels was not accompanied by apparent nerve growth or neurovascular alignment. By day 30, stimulated mesenteric tissues displayed increased vascular density, neural density, and neurovascular alignment across the

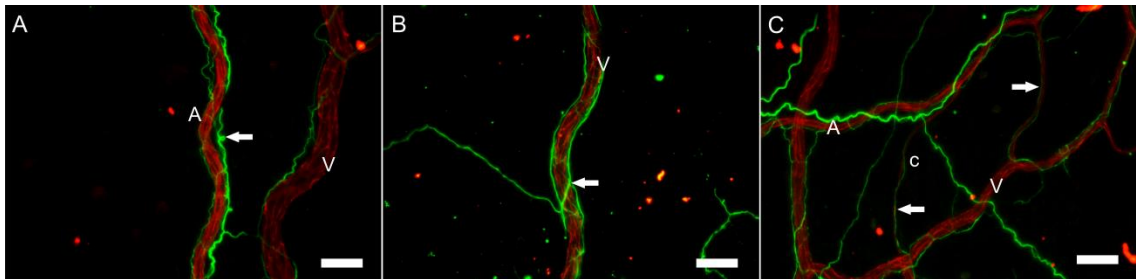


Figure 6: Neurovascular Alignment in Adult Rat Mesentery Window Microvascular Networks. Examples of neurovascular alignment in adult rat mesentery microvascular networks immunolabeled for PECAM (red, endothelial cells) and class III β -tubulin (green, nerves). Neurovascular alignment is observable in unstimulated tissues along arterioles (A), venules (B) and capillary (C). A = Arteriole; V = venule; c = capillary; arrows point to nerves aligned with vessels. Scale bars = 50 μ m. Adapted from Stapor & Murfee [80].

hierarchy of the remodeled vascular network (Figure 8C). Nerves were identified based on morphology and class III β -tubulin positive labeling. Class III β -tubulin positive nerves positively labeled for tyrosine hydroxylase indicating that they are sympathetic nerves (Figure 9). As evidence for the nerves not being sensory, they did not label positively for Substance P (data not shown). Nerve identification using class III β -tubulin was additionally confirmed by immunohistochemical labeling with PGP9.5, NG2 and neurofilament (data not shown).

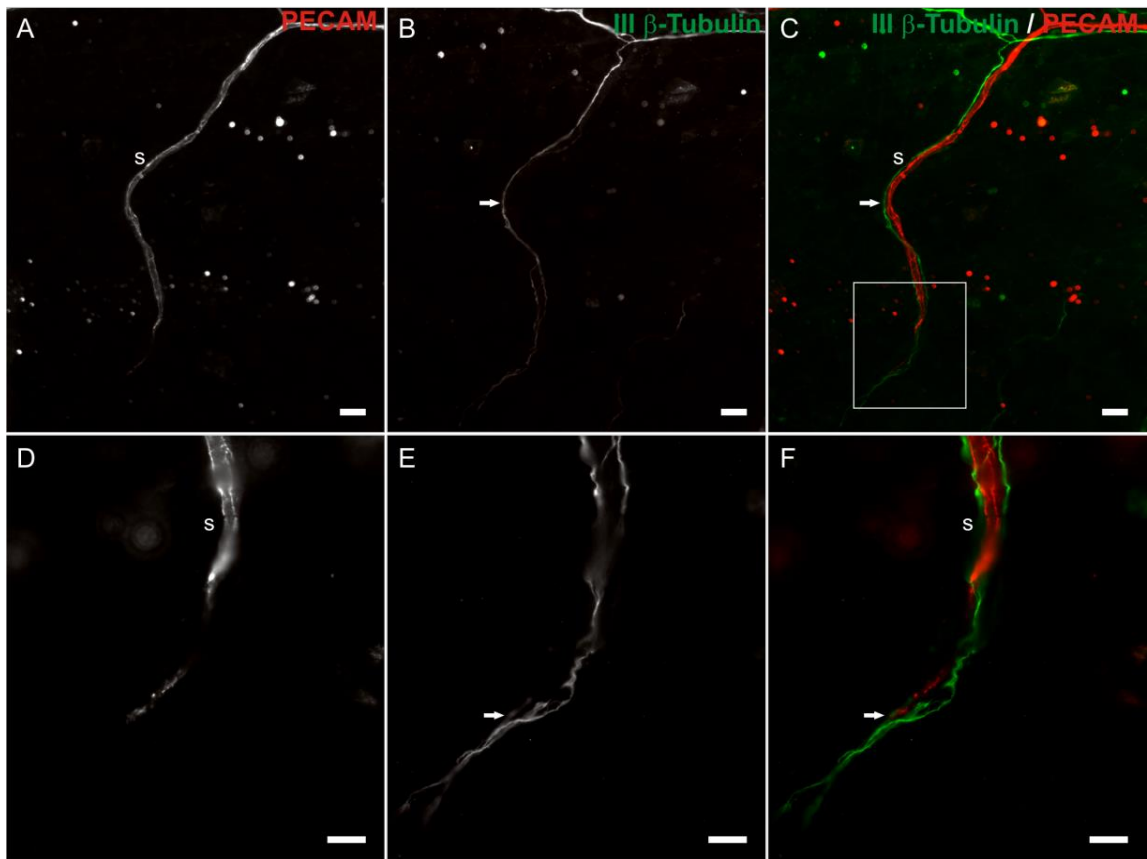


Figure 7: Neurovascular Alignment along Capillary Sprout. Images of alignment of a capillary sprout (s) with a nerve (arrows) immunolabeled for PECAM (A, D; endothelial cells) and class III β -tubulin (B, E; nerves). (A-C) A capillary sprout is aligned with a nerve, which extends past the endothelial tip cell. (D-E) Higher magnification images show that aligned nerves and endothelial cells are within microns, if not closer, for the length of the sprout, including at the tip cell. Adapted from Stapor & Murfee [80].

3.1.2 Neurovascular Alignment during Angiogenesis

Microvascular network growth post 48/80 stimulation is supported by the quantification of vessel segment density per vessel type compared across the time course of initial network growth (Figure 10). Angiogenesis, characterized by sprouts per vascular area, peaked two days post-stimulation. By day 30, capillary sprouting returned to normal levels compared to the unstimulated tissues (Figure 10F). Large arteriole ($> 20 \mu\text{m}$ diameters) densities increased at two days post stimulation, but were similar to unstimulated densities at day 10 and 30 (Figure 10A, D). The density of large venules ($> 20 \mu\text{m}$ diameters) increased by day 2, and returned to the unstimulated level by day 30. The dramatic network growth can be attributed to increased pre-capillary arteriole (10-20 μm), capillary, and post-capillary venule (10-20 μm) densities over the 30 day time course. Segment densities were increased by day 10, and remained elevated by day 30 (Figure 10B, C, E).

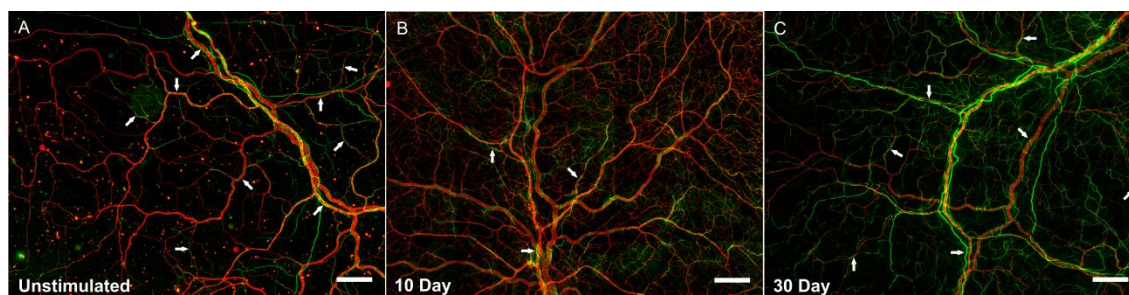


Figure 8: Neurovascular Alignment over 30 Days. Representative montages of adult rat mesentery window microvascular networks (A) unstimulated and (B) 10 days and (C) 30 days post-compound 48/80 stimulation immunolabeled for PECAM (red, endothelial cells) and class III β -tubulin (green, nerves). (A) In unstimulated tissues, PECAM and class III β -tubulin labeling identified aligned vessels and nerves (white arrows). (B) Vascular density increased by day 10, while neurovascular alignment decreased in the network. (C) By 30 days post-stimulation, neurogenesis occurred and neurovascular alignment either increased compared to day 10 or returned to unstimulated levels. Scale bars = 200 μm . Adapted from Stapor & Murfee [80].

The increases in vessel densities 10 days post stimulation were temporally correlated with decreased neurovascular alignment per vessel type. The percentage of vessels aligned

with nerves was determined as the number of vessel segments with nerves aligned, as previously defined, divided by the total number of vessel segments. Ninety percent of large arterioles ($> 20 \mu\text{m}$ diameter) were aligned with nerves in unstimulated tissue. No significant difference was seen across time points (Figure 11A). The percentage of small arterioles ($10\text{-}20 \mu\text{m}$) aligned with nerves decreased from 78% to 45% by 2 days, and to 21% by 10 days. By day 30, 44% of small arterioles were aligned with nerves, yet this percentage was still less than the unstimulated level (Figure 11B). The inverse temporal correlation between vessel growth and nerve alignment over the initial 10 days followed by a returning to unstimulated levels was also characteristic for capillaries, post-capillary venules ($10\text{-}20 \mu\text{m}$) and larger venules ($> 20 \mu\text{m}$ diameter). Capillary alignment with nerves was reduced at 2 and 10 days post stimulation from 45% to 11% and 5%, respectively. Alignment along capillaries increased from 5% on day 10 to 24% by day 30, but still had not returned to alignment percentages observed in unstimulated tissues (Figure 11C). The percentage of large and small venules aligned with nerves decreased by day 10 from 58% and 48% to 24% and 11%, respectively. By day 30, venule alignment percentages returned to statistically similar levels as unstimulated networks

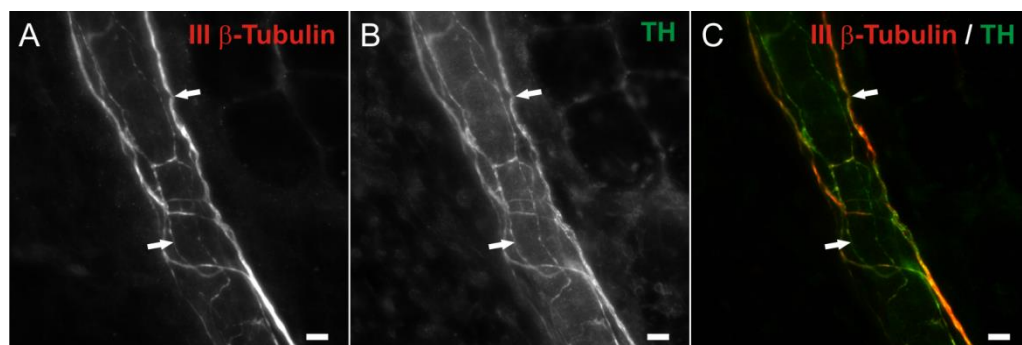


Figure 9: Class III β -Tubulin Co-Labels with Tyrosine Hydroxylase. Representative images of nerves in unstimulated adult rat mesentery tissue immunolabeled with class III β -tubulin (red) and tyrosine hydroxylase (green). Tyrosine hydroxylase identifies the class III β -tubulin positive neurons as sympathetic nerves. Scale bar = $20 \mu\text{m}$. Adapted from Stapor & Murfee [80].

(Figure 11D, E). The percentage of sprouts aligned with nerves was significantly reduced on days 2 and 10 post 48/80 stimulation compared to the unstimulated group and returned to the unstimulated levels by day 30 (Figure 11F).

In order to confirm that neural alignment lags vascular growth during angiogenesis networks was not model specific, we also harvested mesenteric tissues after two alternative stimuli: chronic hypoxia and mesentery exteriorization. For both scenarios, angiogenic networks were characterized by high capillary density and vessel tortuosity and lacked obvious neural/vascular alignment along smaller vessels. These qualitative observations from hypoxia and exteriorization support the quantitative data at day 2 and day 10 presented for the mast cell degranulation model (Figure 12). The chronic hypoxia model represents a more physiological stimulus and is relevant to tissue ischemia scenarios. The exteriorization model represents an alternative inflammatory stimulus [11].

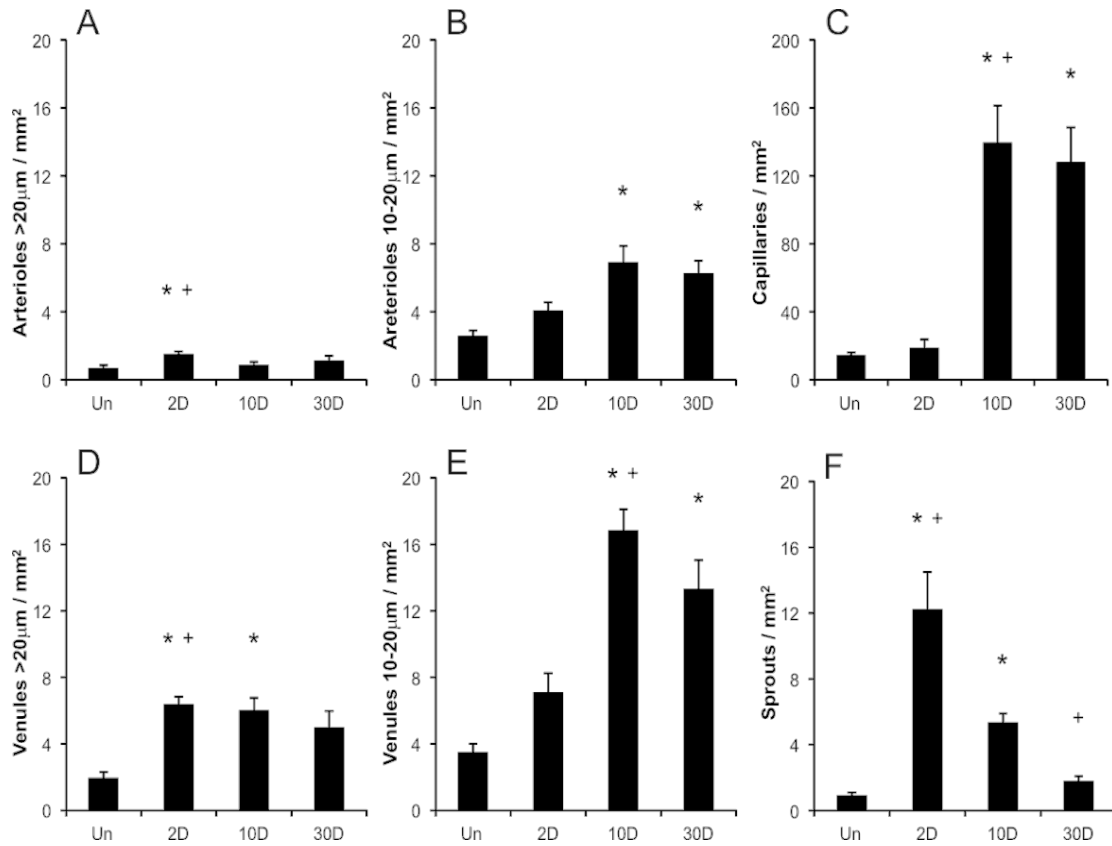


Figure 10: Quantification of Vessel Density. Quantification of vessel segment density in unstimulated microvascular networks (Un), and networks 2, 10 and 30 days post-compound 48/80 stimulation. Vessel densities represented by vessel segment per area (mm^2) were measured for six vessel categories: (A) arterioles > 20 μm , (B) pre-capillary arterioles 10-20 μm , (C) capillaries, (D) venules > 20 μm , (E) post-capillary venules 10-20 μm and (F) sprouts. Statistical comparisons were made using a One-Way ANOVA followed by Tukey's pairwise comparison test. * represents a significant difference compared to unstimulated tissues ($p < 0.05$). + represents a significant difference compared to the previous time point ($p < 0.05$). Values are means \pm SEM. Adapted from Stapor & Murfee [80].

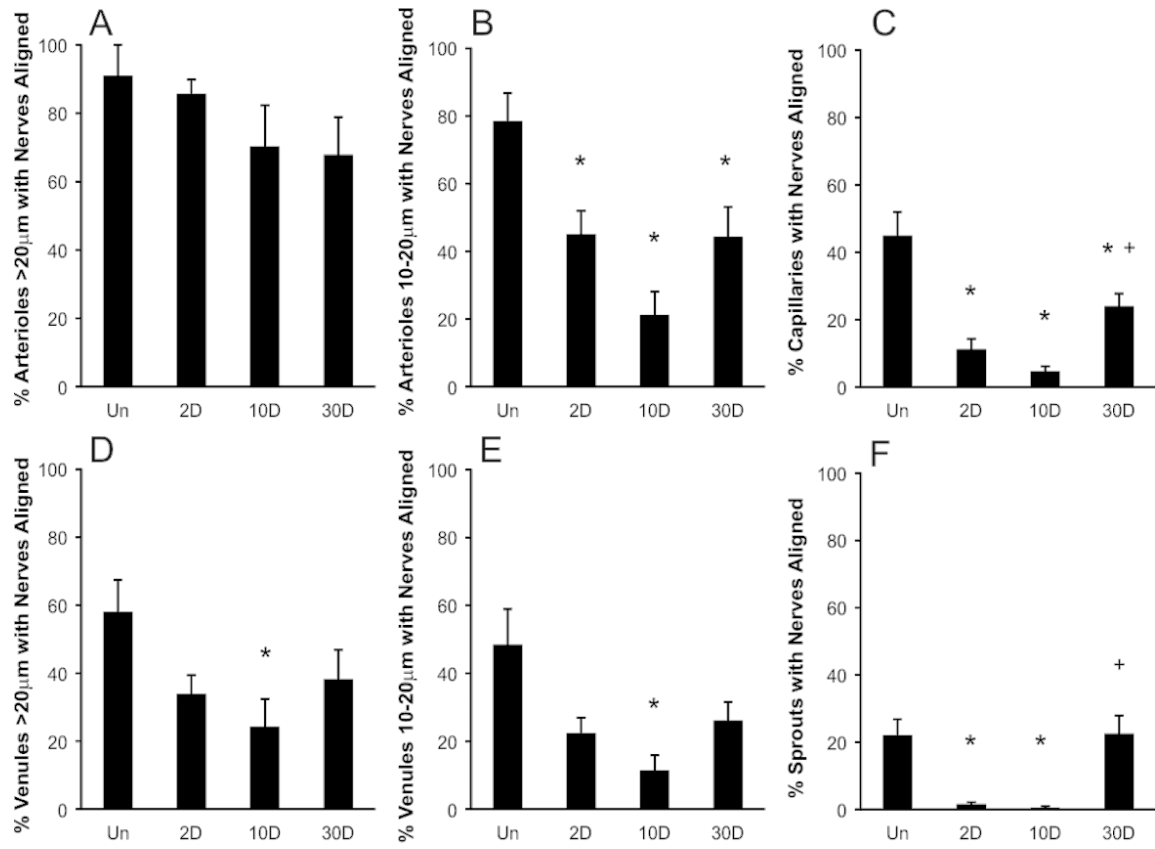


Figure 11: Quantification of Neurovascular Alignment. Quantification of the percentage of vessel segments aligned with nerves in unstimulated microvascular networks (Un), and networks 2, 10 and 30 days post-compound 48/80 stimulation. Neurovascular alignment percentages were determined as the number of segments with a nerve aligned out of the total number of vessel segments, per vessel category: (A) arterioles > 20 µm, (B) pre-capillary arterioles 10-20 µm, (C) capillaries, (D) venules > 20 µm, (E) post-capillary venules 10-20 µm and (F) sprouts. Statistical comparisons were made using a One-Way ANOVA followed by Tukey's pairwise comparison test. * represents a significant difference compared to unstimulated tissues ($p < 0.05$). + represents a significant difference compared to the previous time point ($p < 0.05$). Values are means \pm SEM. Adapted from Stapor & Murfee [80].

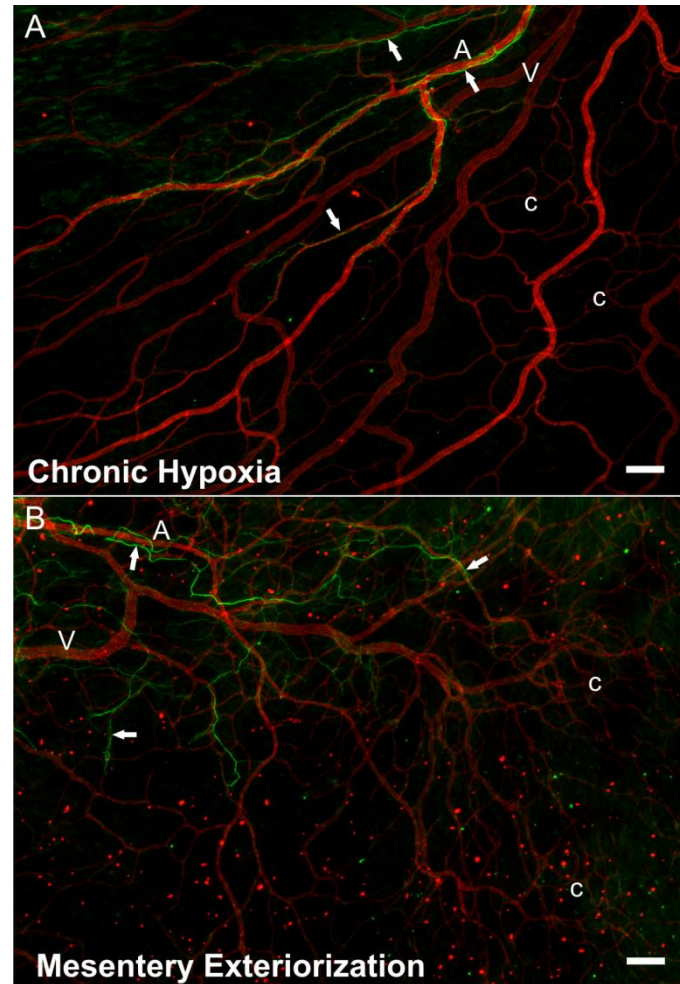


Figure 12: Neurovascular Alignment in Alternative Models of Angiogenesis. Representative montages of mesentery window microvascular networks stimulated by (A) chronic hypoxia and (B) mesentery exteriorization. For chronic hypoxia stimulation of angiogenesis, animals were placed in a chamber maintained at 10% oxygen for 3 days. The mesentery exteriorization model entails exposing 8 mesenteric tissues outside the peritoneal cavity for 20 minutes, and causes an inflammatory response which induces angiogenesis. Both models have been previously documented as angiogenic stimuli [10]. Tissues were immunolabeled for PECAM (red, endothelial cells) and class III β -tubulin (green, nerves). Neurovascular alignment was most prominent in proximal regions of microvascular networks (white arrows). Distal regions of stimulated microvascular networks were void of neurovascular alignment. Scale bars = 100 μ m. Adapted from Stapor & Murfee [80].

3.2 Class III β -Tubulin as a Functional Marker of Perivascular Cells during Angiogenesis

3.2.1 Vascular Expression of Class III β -Tubulin

In adult unstimulated rat mesenteric microvascular networks, class III β -tubulin labeling was observed along nerves. With a few exceptions, class III β -tubulin labeling was not observed along arterioles, venules, and capillaries (Figure 13A). In contrast, two days post 48/80 stimulation, positive class III β -tubulin labeling was observed along the hierarchy of the vascular segments, including arterioles, venules and capillaries (Figure 13B). Class III β -tubulin labeling along vessels was spatially correlated with network regions characterized by capillary sprouting, increased vascular density and vessel tortuosity. Across both unstimulated and stimulated tissues, class III β -tubulin positive labeling was present along a subset of capillary sprouts indicating that its expression is associated with a cellular phenotype present during the sprouting process. Class III β -tubulin positive cells associated with blood vessels exhibited typical perivascular cell morphology (Figure 14 A, B). Along capillaries and capillary sprouts, class III β -tubulin positive pericytes co-labeled for NG2 (Figure 14 C-E) and were longitudinally wrapped around the PECAM positive endothelial cells. Confocal imaging confirmed that class III β -tubulin was not expressed by blood endothelial cells. Along larger arterioles and venules, smooth muscle cells positive for class III β -tubulin were identified based on circumferential wrapping morphologies.

3.2.2 Expression of Class III β -Tubulin during Angiogenesis

Microvascular network growth post 48/80 stimulation was confirmed by the increase in arterial, venous, and capillary segments over the observed 30 day duration (Figure 15A). Angiogenesis, as measured by capillary sprouting per vascular area, peaked by day 2 and returned to normalized levels by day 30. This transient angiogenic time course temporally correlated with class III β -tubulin upregulation along arteriole, venous and capillary segments (Figure 15B). At day 2, 49 \pm 9% of capillaries and 69 \pm 7% of venules and 35 \pm 9% of arterioles were covered with class III β -tubulin labeling perivascular cells. Similar to the metric for capillary sprouting, by day 30 positive labeling along capillaries had returned to unstimulated levels. At day 30 the percentages of arterioles and venules with class III β -tubulin labeling were decreased compared to their previous time points, yet still not back to unstimulated levels indicating that remodeling of larger vessels persists past the time course for sprouting. The percentages of capillary sprouts with class III β -tubulin labeling pericytes were comparable across experimental groups.

Examples of class III β -tubulin upregulation by angiogenic perivascular cells were also observed in remodeling mesenteric networks stimulated by chronic hypoxia and tissue exteriorization (Figure 16).

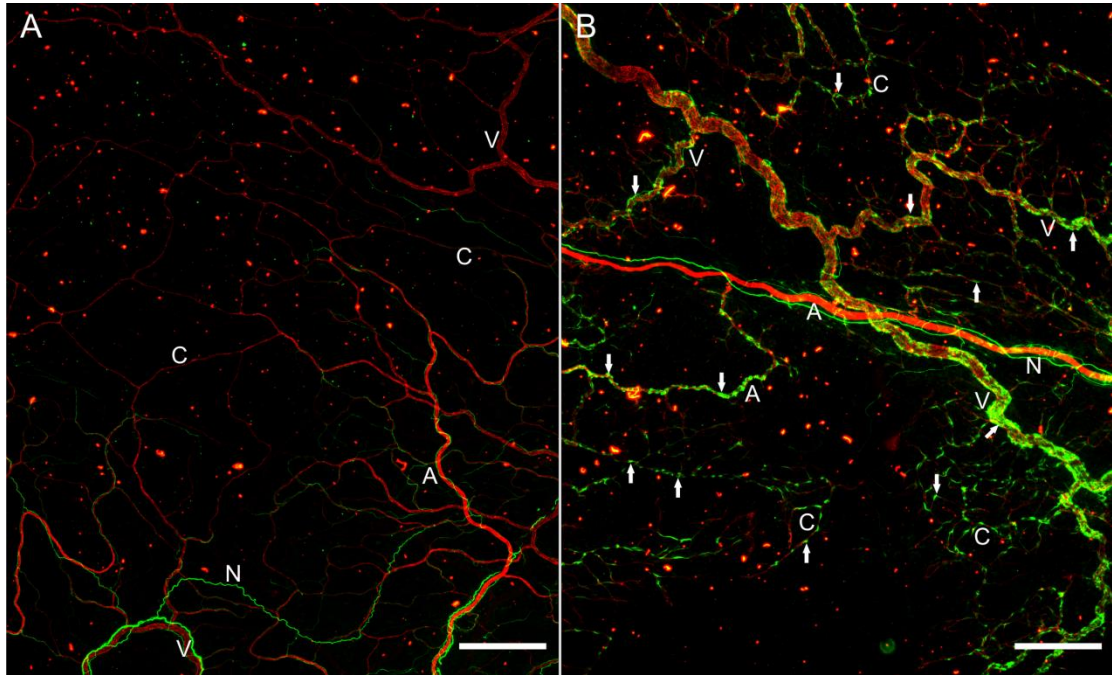


Figure 13: Class III β -Tubulin Expression during Angiogenesis. Representative montages of unstimulated (A) and compound 48/80 stimulated (B) adult rat mesentery window microvascular networks immunolabeled for PECAM (red) and class III β -tubulin (green). (A) In unstimulated tissues, class III β -tubulin+ labeling identified nerves and was not observable in vascular cells along arterioles, capillaries, and venules. (B) At 2 days post-stimulation, class III β -tubulin labeling identifies vascular pericytes along vessels spatially correlated with characteristics of network growth including increased capillary sprouting, vessel density, and vessel tortuosity (A: arteriole, C: capillary, V: venule, N: nerve; arrows indicate examples of class III β -tubulin+ perivascular cells). Scale bars = 200 μ m. Adapted from Stapor & Murfee [75].

3.2.3 Effects of Class III β -Tubulin Inhibition on Pericyte Proliferation and

Migration

Human brain derived vascular pericytes expressed class III β -tubulin *in vitro* (Figure 17).

Suppression of class III β -tubulin expression by siRNA was confirmed by

immunolabeling for the protein 72 hours after transfection was initiated (Figure 17). The

percentage of Ki67 positive nuclei was assessed to indicate the proportion of cells

actively proliferating. While the Control Sham and Control siRNA groups did not differ

significantly, class III β -tubulin inhibition reduced the percentage of Ki67 positive cells

by about 10% (Figure 18; $p < 0.001$ vs. Control Sham and Control siRNA). The results

suggest that class III β -tubulin suppression reduces the proliferative capability of human brain vascular pericytes.

Pericyte migration was assessed using a scratch test. Cells were grown to confluence and scratched 72 hours after transfection was initiated. Scratch areas did not significantly differ at the time of the scratch, as indicated by a one way ANOVA test (data not shown). After 6 hours, Control Sham scratches were $94.5 \pm 3\%$ closed, and did not significantly differ from Control siRNA groups, which closed $89.8 \pm 12\%$ closed. Class III β -tubulin inhibition resulted in a significant reduction in wound closure to only $67.4 \pm 7.9\%$ (Figure 19; $p < 0.001$). Paclitaxel treatment inhibited scratch closure in all groups. Control Sham and Control siRNA paclitaxel treated groups did not significantly differ with $31.7 \pm 7.5\%$ and $26.1 \pm 4.7\%$ scratch closure, respectively. However, class III β -tubulin inhibition resulted in a significant reduction in scratch closure again with only $15.6 \pm 5\%$ scratch closure (Figure 19; $p < 0.001$). The reduction in scratch closure in the class β -tubulin siRNA group compared to Control siRNA was approximately -22.4%. In the presence of paclitaxel, this reduction was exaggerated to approximately -40.2%, suggesting that class III β -tubulin suppression may also sensitize pericytes to paclitaxel treatment.

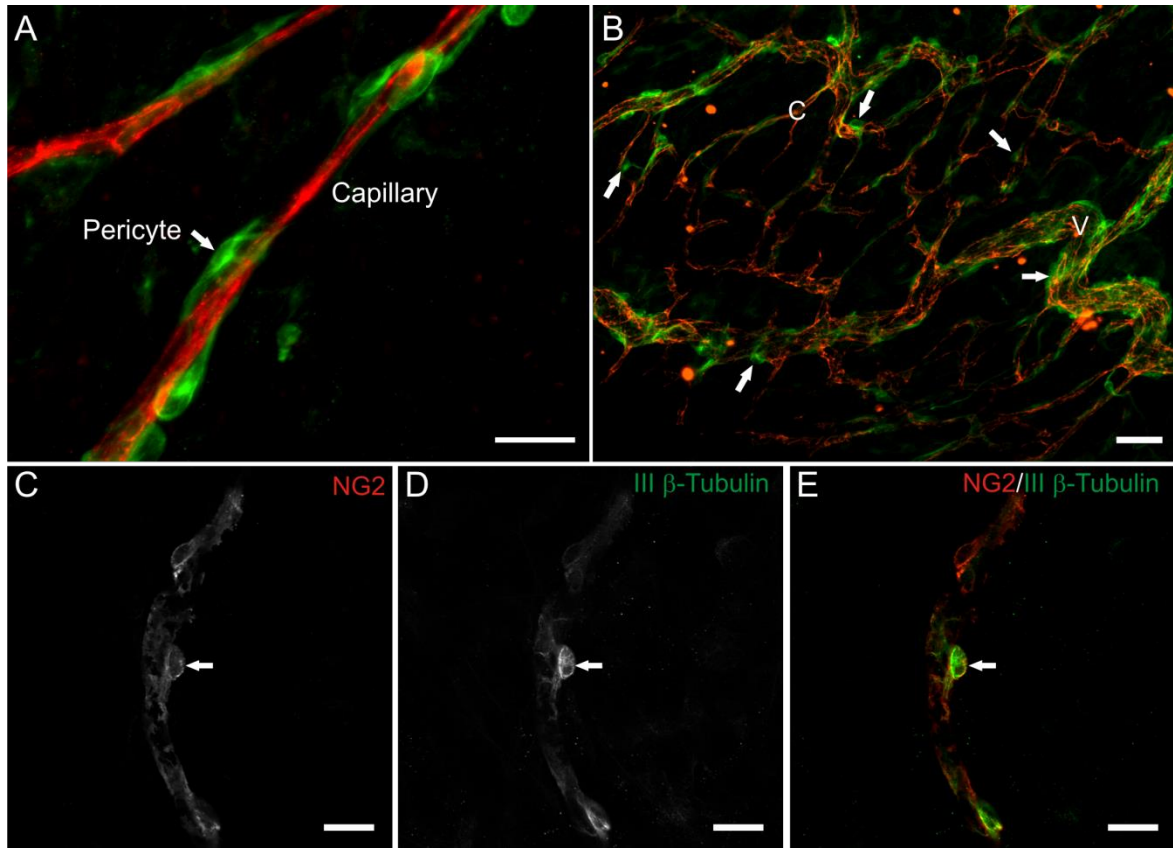


Figure 14: Class III β -Tubulin Expression by Pericytes. Examples of class III β -tubulin+ pericyte morphology, location and co-localization with NG2 proteoglycan. (A) Image of a class III β -tubulin+ (green) pericyte characteristically wrapped around a PECAM+ (red) capillary. (B) Image of class III β -tubulin+ (green) labeling of pericytes along PECAM+ (red) labeling of vessels in a remodeling region, classified by high capillary density, capillary sprouting, and tortuous vessels (C: capillary, V: venule; arrows indicate examples of class III β -tubulin+ perivascular cells). (C-E) Example of co-localization of class III β -tubulin (D, green) with NG2 proteoglycan (C, red) confirms class III β -tubulin labeling of perivascular cells. Scale bar = 20 μ m (A), 50 μ m (B) and 20 μ m (C). Adapted from Stapor & Murfee [75].

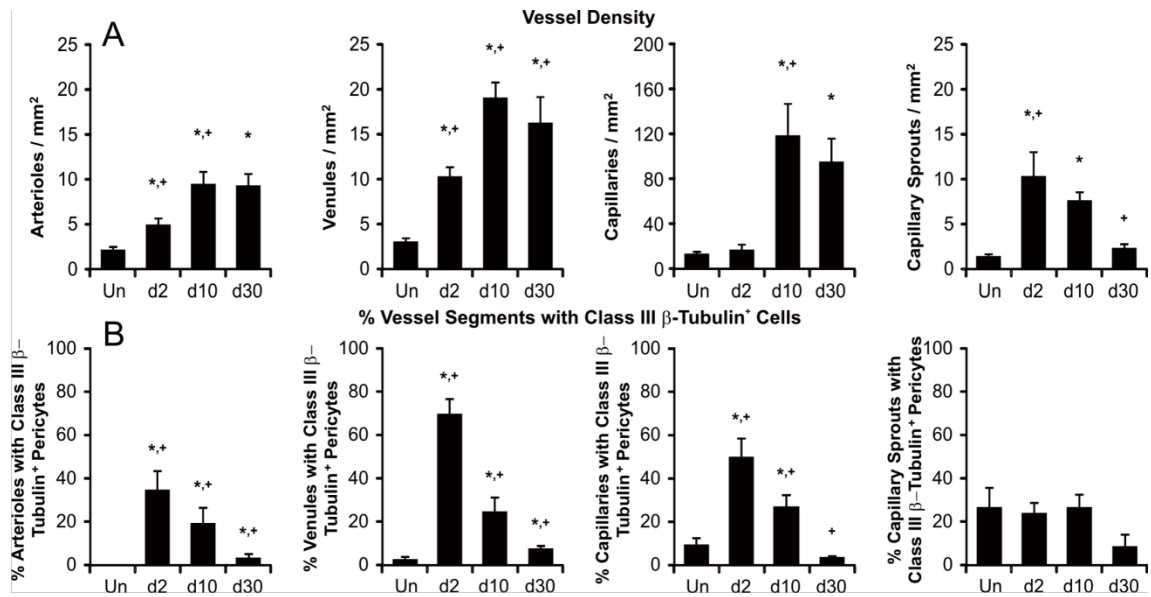


Figure 15: Quantification of Class III β -Tubulin Expression by Pericytes. Quantification of vessel segment density and the percentage of vessel segments with class III β -tubulin+ pericytes in unstimulated microvascular networks (Un), and networks 2, 10 and 30 days post-compound 48/80 stimulation. (A) Vessel densities represented by vessel segment per area (mm^2) across arterioles, venules, capillaries and capillary sprouts for each time point. (B) Percentage of vessel segments with class III β -tubulin+ perivascular cell coverage across arterioles, venules, capillaries and capillary sprouts for each time point. * represents a significant difference compared to unstimulated tissues ($p < 0.05$). + represents a significant difference compared to the previous time point ($p < 0.05$). Values are means \pm SEM. Adapted from Stapor & Murfee [75].

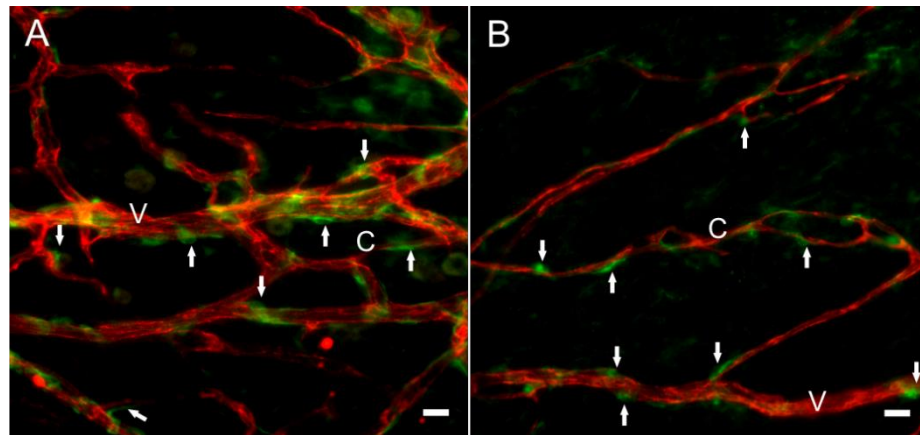


Figure 16: Class III β -Tubulin Expression in Alternative Models of Angiogenesis. Examples of class III β -tubulin+ pericyte expression in alternative models of angiogenesis. (A) Image of class III β -tubulin+ (green) pericytes 3 days post-stimulation by the tissue exteriorization model. (B) Image of class III β -tubulin+ (green) pericytes 3 days post-stimulation by systemic hypoxia. (C: capillary, V: venule; arrows indicate examples of class III β -tubulin+ perivascular cells). Scale bar = 50 μ m. Adapted from Stapor & Murfee [75].

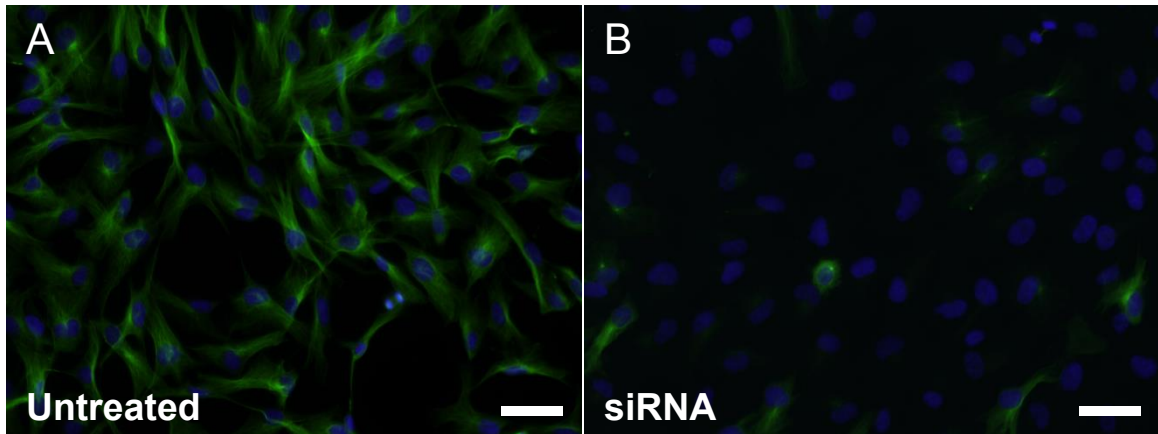


Figure 17: Human Pericyte Expression of Class III β -Tubulin. Images of class III β -tubulin positive expression *in vitro* by human brain-derived vascular pericytes. (A) Cultured hBVPCs express class III β -tubulin (green). (B) Suppression of class III β -tubulin was confirmed by immunolabeling of pericytes 72 hours after transfection shown by nuclei (blue) which are class III β -tubulin negative. Scale bar = 50 μ m.

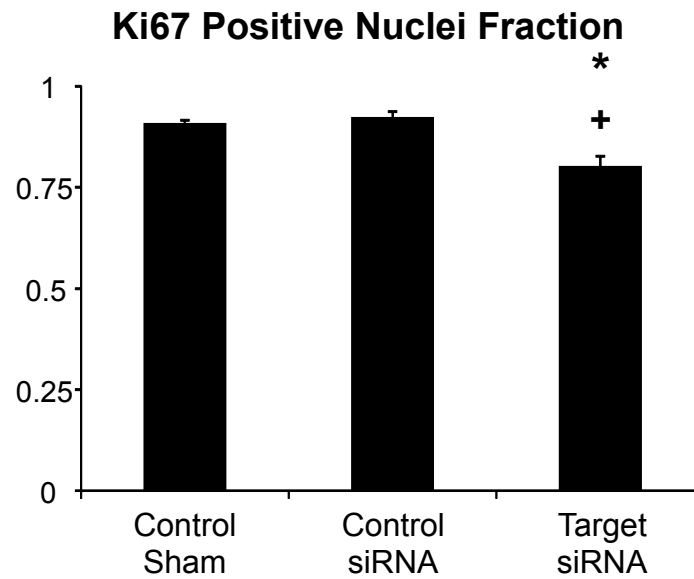


Figure 18: Quantification of Proliferation. Quantification of the fraction of Ki67+ hBVPC nuclei indicated the proportion of cells that are proliferating. * represents significant difference compared to Control Sham ($p < 0.001$). + represents significant difference compared to Control siRNA ($p < 0.001$).

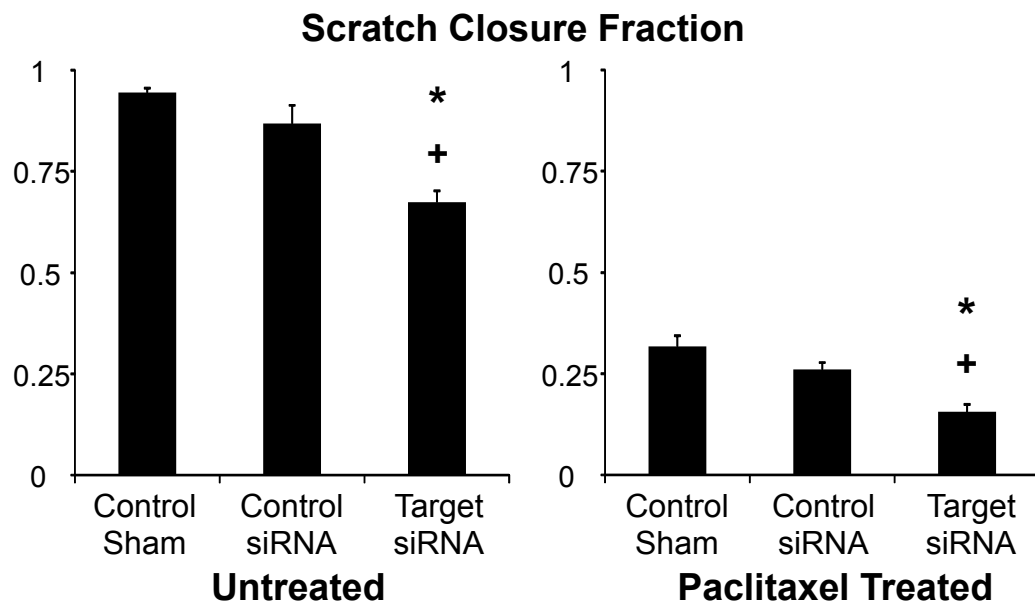


Figure 19: Quantification of Migration. Quantification of the fraction of scratch closure after 6 hours for untreated and paclitaxel treated hBVPCs. * represents significant difference compared to Control Sham ($p < 0.001$). + represents significant difference compared to Control siRNA ($p < 0.001$).

3.3 The Adult Rat Mesentery as a Model for Multicellular and Multisystem

Interactions during Angiogenesis

3.3.1 Assessment of Microvascular Viability, Morphology and Phenotype

Microvascular networks displayed hierarchical branching patterns after being cultured for 3 days [3]. These networks consisted of arterioles, capillaries, and venules. PECAM, SM α -actin, and NG2 labeling identified the presence of endothelial cells, smooth muscle cells and pericytes, respectively (Figure 20). Arterioles compared to paired venules displayed increased SM α -actin cell wrapping (Figure 20A-B). NG2 labeling of smooth muscle cells along larger vessels has been previously shown to be arterial versus venule specific [11]. In the cultured mesenteric tissues, we also observed arterial specific NG2 smooth muscle cell labeling (Figure 20C). These observations provide an example of differential arterial/venous identity in an adult microvascular network in the absence of hemodynamic forces and motivate future investigations aimed at elucidating the functional role of NG2 as an arterial/venous marker. NG2 positive pericytes along capillaries exhibited a typical elongated morphology (Figure 20D). After 3 days in culture the percentage of NG2 positive vessel segments per vessel type (arterioles, venules, or capillaries) were statistically comparable (Figure 20E) indicating that perivascular cells remain differentiated for at least 3 days.

Lymphatic networks and nerves also remain present. Lymphatic versus blood vessel identity was confirmed based on endothelial cell morphology, PECAM labeling intensity,

and labeling with LYVE-1 (Figure 21A-C). Nerves were distinguished from blood vessels based on morphology and labeling with class III β -tubulin (Figure 21D-F). Tissues remained viable after being cultured in serum free MEM for 7 days (Figure 22A-C). Live cells were present throughout the tissue and along branching structures consistent with microvessels. Co-localization of live cells with microvessels was confirmed by co-labeling with calcein and BSI-lectin (data not shown). After 7 days in culture, LYVE-1 positive lymphatic vessels remain present (Figure 22D-F), yet the

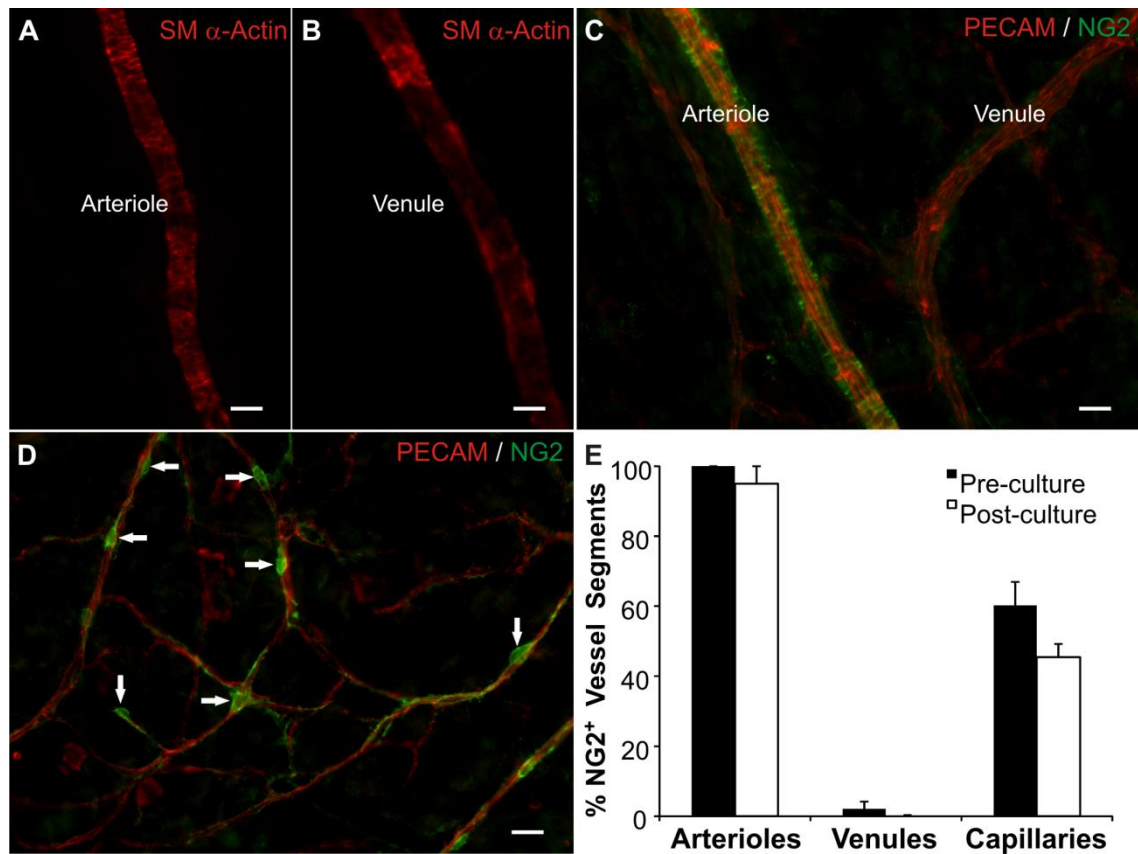


Figure 20: Mural Cells in the Mesentery Culture Model. Vascular cells remain present and maintain morphological and phenotypic characteristics in the rat mesentery tissues cultured in serum free media for 3 days. After 3 days in culture, (A) arterial and (B) venous smooth muscle cells are identified by smooth muscle α -actin immunolabeling and display respective arterial and venous morphologies. (C) NG2 and PECAM labeling of a paired arteriole and venule. NG2 labeling displayed an arterial-specific smooth muscle cell identity. (D) NG2 and PECAM labeling along capillaries. NG2 positive cells exhibited typical pericyte morphology (arrows). (E) Quantitative comparison of the percentage of vessels with NG2 positive cells in freshly harvested tissues (pre-culture) and tissues cultured in MEM for 3 days (post-culture). Values are mean \pm s.e.m. Scale bars = 25 μ m. Adapted from Stapor et al. 2013 [104].

number of NG2 positive perivascular cells is reduced indicating the potential for cell de-differentiation during culture experiments longer than 3 days (Figure 22G-I).

3.3.2 Stimulation of Capillary Sprouting at Specific Vessel Locations

Culturing rat mesenteric tissues in MEM plus bFGF or MEM plus VEGF for 3 days stimulates angiogenesis. Compared to the respective MEM alone control groups, the angiogenic groups displayed an increase in capillary sprouting (Figure 23). Capillary sprouting was associated with endothelial cell proliferation (data not shown). Both the presence of bFGF (Figure 24C) and VEGF (Figure 24F) caused an increase in the number of capillary sprouts per capillary segment. However, only bFGF caused a statistically significant increase in the number of capillary sprouts off venules greater than 20 μm (Figure 24B,E). Per growth factor, a significant increase in capillary sprouting along arterioles was not observed (Figure 24A,D). These results demonstrate that capillary sprouting in this model preferentially occurs along specific vessel types (capillaries and venules), a phenomenon consistent with the *in vivo* observations [3]. The number of arterioles, venules, and capillary segments normalized per vascular area were not significantly different across MEM alone and MEM plus growth factor groups (data not shown).

3.3.3 Regulation of Capillary Sprouting by Endothelial Cell-Pericyte Interactions

Angiogenesis involves both endothelial cells and pericytes [4]. As an example, NG2, a membrane spanning chondroitin sulfate proteoglycan expressed by pericytes, has recently been shown to be a regulator of endothelial cell proliferation and migration associated

capillary sprouting [55,84]. The inclusion of NG2 antibody in the bFGF supplemented MEM prevented an increase in capillary sprouting in the mesentery culture model (Figure 23D, 24B,C). The density of capillary sprouts off venules and capillaries was decreased for the bFGF plus NG2 antibody group versus bFGF alone and the bFGF plus rabbit IgG groups. The density of capillary sprouts off capillaries was also decreased for the VEGF plus NG2 antibody group (Figure 24F). NG2 positive perivascular cell targeting was confirmed by secondary-only labeling at the end of the experiment (Figure 25). Tissues were labeled for PECAM and a secondary antibody to target the rabbit derived NG2 antibody. The lack of secondary labeling in the RIgG + VEGF group serves as a control for NG2 Ab specificity and antibody targeting.

3.3.4 Modulation of Lymphatic/Blood Endothelial Cell Interactions during Angiogenesis

The rat mesentery culture model also enables the investigation of lymphatic/blood endothelial cell interactions during angiogenesis. Angiogenesis and lymphangiogenesis are known to share common signaling cues [85,86]. Our laboratory discovered the presence of physical lymphatic/blood endothelial cell connections in adult rat mesenteric microvascular networks [79]. In the present study, we show that the occurrence of these physical interactions can be influenced by specific growth factors (Figure 26). VEGF caused an increase in the number of lymphatic/blood endothelial cell connections per vascular area compared to the MEM alone control group, while bFGF did not (Figure 26C). Observation of sub 0.7 μm optical sections using confocal microscopy confirmed PECAM labeling continuity along endothelial cells at connections sites (Figure 26A,B).

Lymphatic vessel identity at sites of connection was verified with LYVE-1 labeling (Figure 26D-F). Evidence for lymphangiogenesis in our model is supported by the observation of LYVE-1 positive endothelial cell extensions in tissues cultured for 3 days in MEM plus bFGF (Figure 27).

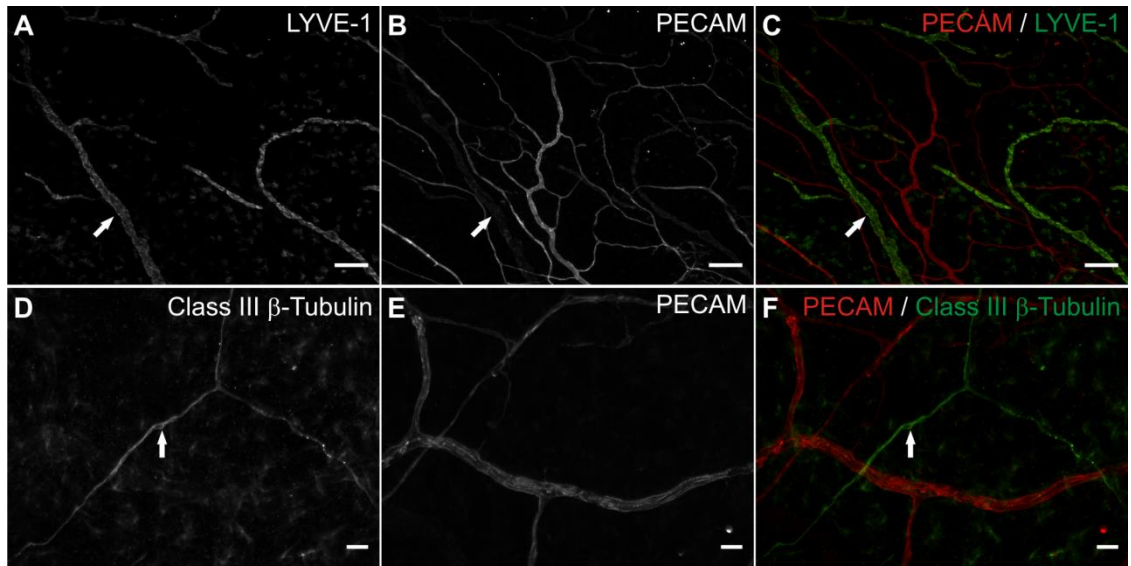


Figure 21: Lymphatics and Nerves in the Mesentery Culture Model. Lymphatic and neural systems remain present in the rat mesentery culture model in serum free media for 3 days. (A-C) LYVE-1 and PECAM immunolabeling identified intact lymphatic networks (arrows) after 3 days of culture in serum free media. (D-F) Class III β -tubulin and PECAM immunolabeling. After 3 days of culture in serum free media. Positive class III β -tubulin immunolabeling identified nerves (arrows). Scale bars = 200 μ m (A-C), 25 μ m (D-F). Adapted from Stapor et al. 2013 [104].

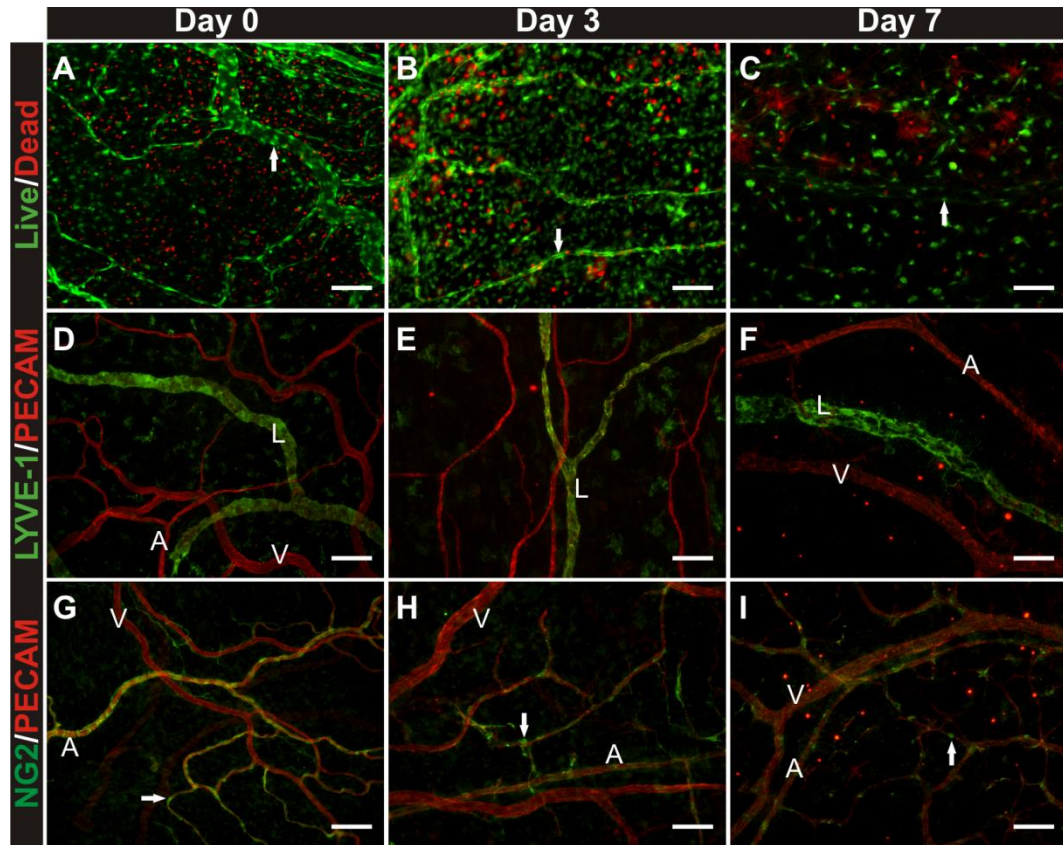


Figure 22: Cell Viability in the Mesentery Culture Model. Evaluation of tissue viability and vascular cell phenotypes pre-culture, and 3 and 7 days in culture with serum free media. (A-C) Cell viability/cytotoxicity labeling. Arrows indicate apparent live vascular structures. (D-F) LYVE-1 and PECAM immunolabeling. (G-I) NG2 and PECAM immunolabeling. Arrows indicate pericytes. By day 7, the majority of arterioles lose NG2 positive cell coverage. NG2 positive cells were still observable along capillaries, yet the percentage of capillaries with pericytes is decreases. (A) indicates arteriole. (V) indicates venule. (L) indicates lymphatic. Scale bars = 50 μm . Adapted from Stapor et al. 2013 [104].

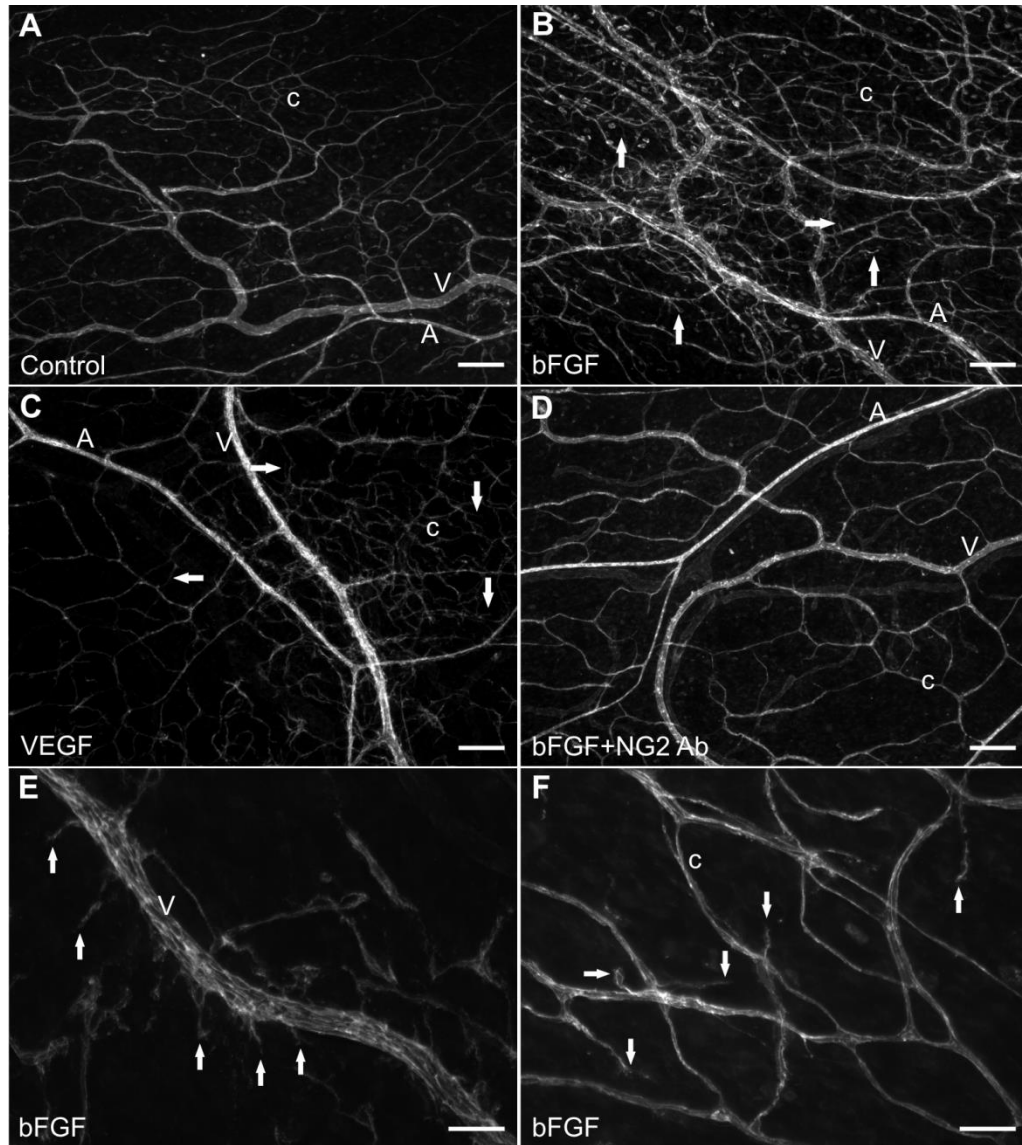


Figure 23: Angiogenesis in the Mesentery Culture Model. Microvascular networks can be stimulated to undergo angiogenesis while in culture for 3 days. Networks after 3 day culture in (A) Serum free MEM, (B) MEM plus bFGF, (C) MEM plus VEGF, (D) MEM plus bFGF and NG2 antibody. (E, F) Higher magnification images of capillary sprouts (arrows) off a venule and existing capillaries. (A) indicates arteriole. (V) indicates venule. (c) indicates capillary. Scale bars = 200 μm (A-D), 50 μm (E, F). Adapted from Stapor et al. 2013 [104].

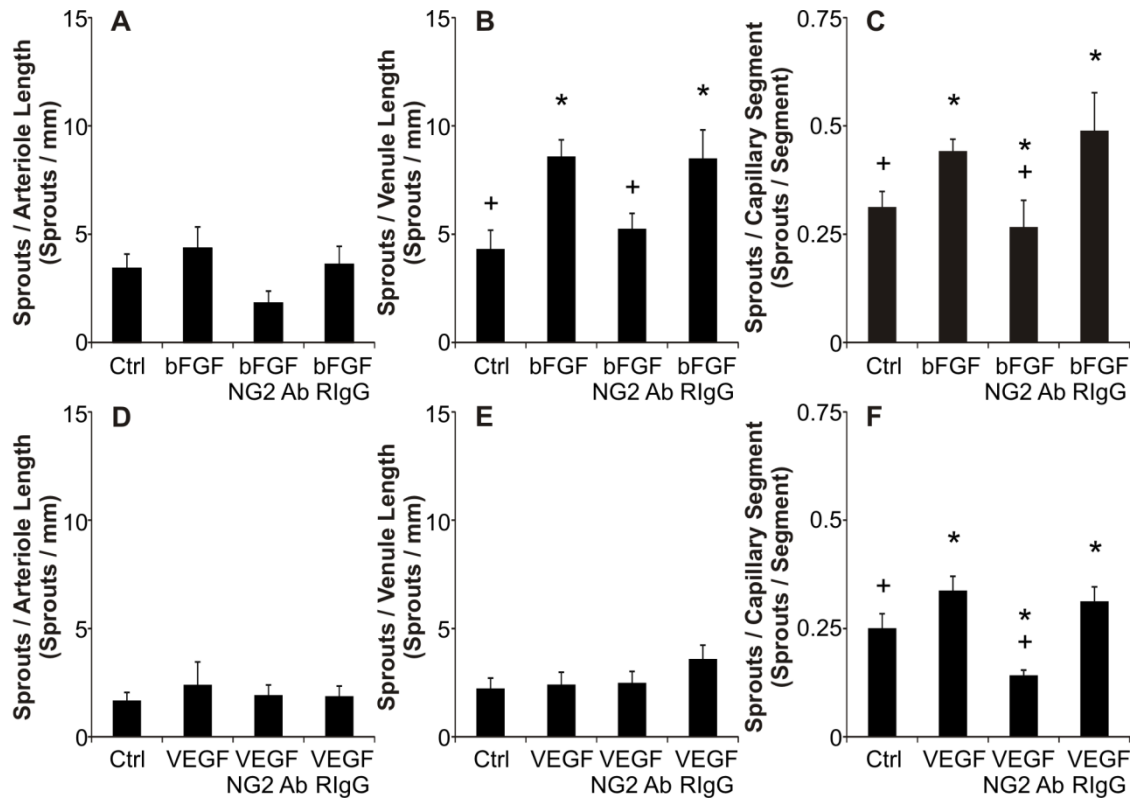


Figure 24: Quantification of Angiogenesis. Quantification of capillary sprouting per vessel type after (A-C) bFGF and (D-F) VEGF stimulation. For each growth factor stimulation experiment the numbers of sprouts per vessel type length after 3 days in culture were compared across experimental groups: control (MEM alone), MEM + growth factor (GF), MEM + GF + NG2 antibody, and MEM + GF + Rabbit IgG. The rabbit IgG groups controlled for potential non-specific antibody binding effects. * indicates significance against the control group ($p < 0.05$). + indicates significance against the growth factor group ($p < 0.05$). Values are mean \pm s.e.m. Adapted from Stapor et al. 2013 [104].

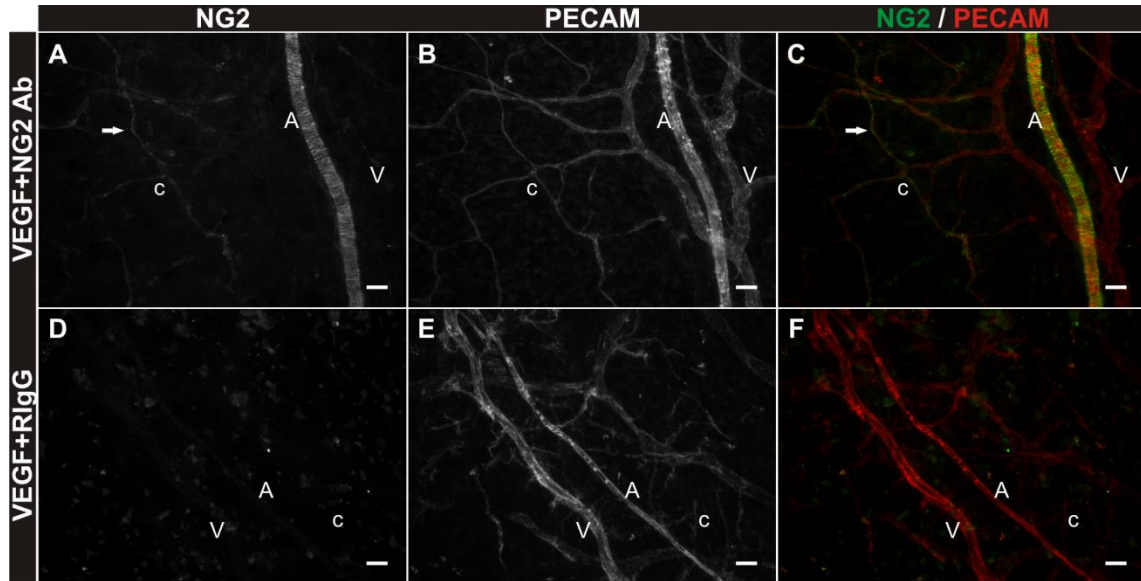


Figure 25: NG2 Targeting. Confirmation of antibody targeting NG2 positive cells over the culture time course. (A-C) NG2 and PECAM labeling of rat mesenteric tissues post 3 days in culture in MEM + VEGF + NG2 antibody. Anti-rabbit IgG secondary labeling at day 3 identifies NG2 positive smooth muscle cells tightly wrapped around PECAM positive arterioles and pericytes (arrows) elongated along PECAM positive capillaries. (D-F) NG2 and PECAM labeling in tissues cultured in MEM + VEGF + Rabbit IgG antibody. Secondary antibody labeling targeting bound rabbit derived protein is absent in field of views containing PECAM positive vessels. (A) indicates arteriole. (V) indicates venule. (c) indicates capillary. Scale bars = 25 μ m. Adapted from Stapor et al. 2013 [104].

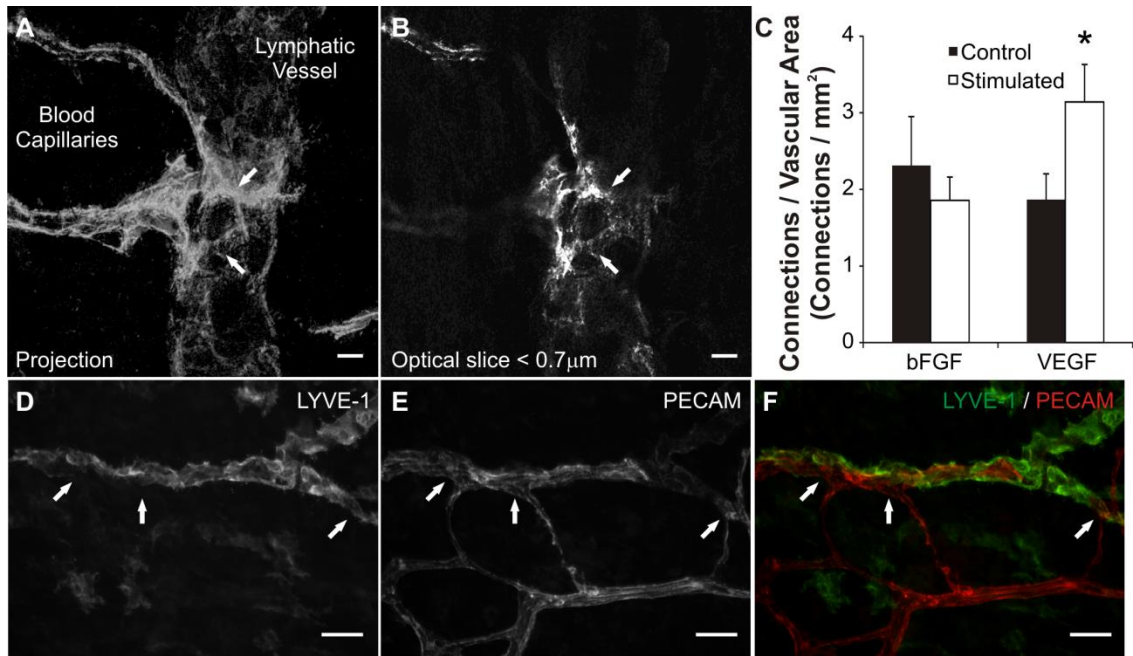


Figure 26: Lymphatic Connections in the Mesentery Culture Model. (A) Confocal projection of sub 0.7 μm slices displays lymphatic/blood endothelial cell connections (arrows) identified by continuous PECAM labeling across cell types. Continuous PECAM labeling was confirmed by observation of each individual optical slice (B) throughout the thickness of the vessels at the connection site. (C) Quantification of connections per vascular area for bFGF and VEGF stimulated networks. VEGF stimulated an increase in connection density compared to control tissues. The density of connections did not change between unstimulated and bFGF stimulated tissues. * indicates significance against the control group ($p < 0.05$). (D-F) LYVE-1 and PECAM labeling of lymphatic and blood vessels at connection sites (arrows). Scale bars = 10 μm (A, B), 50 μm (D-F). Adapted from Stapor et al. 2013 [104].

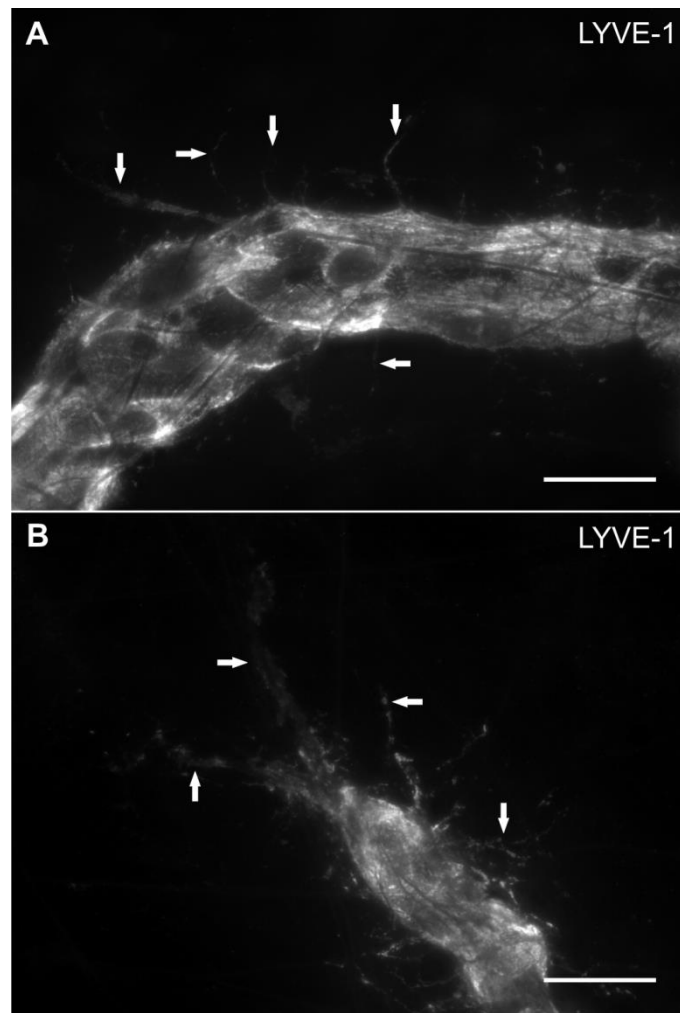


Figure 27: Lymphangiogenesis in the Mesentery Culture Model. Examples of LYVE-1 positive filopodia (arrows) extending from lymphatic vessels at different locations within a lymphatic network stimulated by 3 day culture in MEM plus bFGF. (A) Extensions off a lymphatic vessel segment. (B) Extensions off a blind ended lymphatic vessel. Scale bars = 25 mm. Adapted from Stapor et al. 2013 [104].

CHAPTER 4: DISCUSSION

4.1 Spatiotemporal Relationship between Angiogenesis and Neurovascular

Alignment

The primary finding of this aim is that neurovascular alignment follows microvascular growth in adult rat mesentery microvascular networks. Neurovascular alignment has been previously observed in the rat mesentery down to pre-capillary arterioles and post-capillary venules [87]. We show that alignment is also present throughout the network down to the capillary level indicating that nerves do associate with blood vessels along all microvascular vessel types (Figure 6, 11). Post 48/80 stimulation, mesenteric microvascular network growth is characterized by a dramatic increase in angiogenesis and subsequent increases in the densities of arterioles, capillaries, and venules. Initial network growth is then followed by neurovascular alignment.

The link between neural and vascular patterning has recently emerged as a new area of microvascular research. At the molecular level, the link is supported by shared signaling mechanisms including, ephs/ephrins, semaphorins/neuropilins (NPs) and plexins and netrins/DCC and Unc5 receptors, as well as multiple growth factors [19,22,88]. However, the spatial relationships between both systems in adult tissues and during angiogenesis remain unclear. In embryonic mouse limb skin, neural-derived VEGF directs arterialization through the neuropilin 1 receptor after a capillary bed has been established

[28]. VEGF derived from arteries also coordinates growth of motor neurons and sympathetic innervation [89,90]. All together, the coordinated growth mechanisms involved in neurovascular alignment are just beginning to be understood. Insight can be gained by examining the spatial interactions between the two systems across different vessel types within adult microvascular networks. In 2005, Bearden and Segal showed that somatic motor nerves in adult mouse skeletal muscle align with 15-60 μm diameter arterioles [91]. These observations are in agreement with our results that nerves align with arterioles in rat mesenteric microvascular networks. We also show that nerves are capable of aligning with microvessels across the hierarchy of a network, including venules and capillaries.

In adult tissue denervation and sympathectomy models, nerves use vessels as guides while reinnervation occurs [89,90]. During remodeling associated with skin and neuronal grafts, neovascularization precedes neural growth [29,30,92]. Our results provide additional support for neurovascular alignment trailing angiogenesis and add a valuable view of these dynamics across the hierarchy of an intact microvascular network.

Sympathetic nerves in adult rat mesenteric networks have been shown to influence vessel diameter [93]. Furness and Marshall paravascular nerve stimulation affected the diameters of terminal arterioles and larger arterioles, but not pre-capillary arterioles. On the venule side, only venules greater than 30 μm were affected by paravascular nerve stimulation. These results and our observations of nerves present along a percentage of smaller arterioles and venules in unstimulated motivate the need for future investigations

aimed at determining whether nerve presence necessarily correlates with neuronal function. Our characterization of neurovascular alignment over the time course of microvascular network growth also motivates future studies to determine when do new nerves become functional.

The rat mesentery represents a model to study the interaction of multiple cell types involved in microvascular remodeling [11,40]. It allows for observation across the entire hierarchy of intact microvascular and neural networks down to the cellular and sub-cellular level at different time points during microvascular remodeling. Unstimulated tissues display nominal levels of angiogenesis intrinsic to physiological vascular network expansion within mesenteric windows. In this study we stimulated rapid network growth via compound 48/80 injections to compare with unstimulated networks. Compound 48/80 stimulation produces a robust angiogenic response through mast cell activation and histamine release, followed by further network remodeling [73,74]. The initial increase in capillary sprouting by day 2 corresponds with the subsequent density increases for pre-capillary arterioles, capillaries, post-capillary venules and venules by day 10. As evident by increases in vascular density upstream and downstream of the capillary level, 48/80 stimulated angiogenesis is followed by arteriogenesis. Over the 30 day time course of network growth, the densities for the largest arterioles and venules transiently increases. By day 30 for venules and by day 10 for arterioles, vessel density is not statistically different from unstimulated levels. A possible explanation for these transient increases is vessel dilation, which is a characteristic of angiogenesis [94]. During angiogenesis, which peaks at day 2 in our model, dilation of smaller vessels could cause them to be counted as

larger vessels. At later time points (i.e. day 30) when angiogenesis has returned to unstimulated levels, these vessels might then be classified as smaller vessels again.

The relative distribution of nerve alignment along the growing networks implicates a role for nerves in the vessel maturation process rather than initial growth. To examine this potential correlation between perivascular cell and nerve recruitment, we additionally examined nerve and perivascular cell presence at 10 days post compound 48/80 stimulation (data not shown). The majority of the SM α A positive vessels were not associated with nerves. These observations indicate that the recruitment of SM α A positive cells is not dependent on innervation. The presence of perivascular cells prior to nerve alignment is consistent with a role for perivascular cells in nerve recruitment and their ability to secrete NGF, a potent neurotrophic factor, which promotes sympathetic innervation of the microvasculature [95,96].

We selected diameter categories for our study in order to capture potential differences in nerve/blood vessel alignment in different regions of a network. In particular, we focused on the capillary level, the pre- or post-capillary level, or along larger vessels. Relative vessel diameter binning is justified because we used a consistent fixation method. However, tissue fixation could influence nominal diameter measurements. In our laboratory, we have shown that Methanol fixation could indeed influence vessel diameter (data not shown). Feeding mesenteric arterioles in the Methanol fixation group were smaller when compared to vessels fixed with paraformaldehyde. The diameters of venules fixed in methanol were significantly smaller than those that were unfixed or fixed

with either paraformaldehyde. In the context of our results, the potential effect of decreased diameter measurements due to Methanol fixation would have caused for larger vessels to be potentially counted in the pre-/post-capillary vessel category. Given that in general larger vessels are more aligned with nerves, this potential shift in vessel count would have caused an apparent increase in alignment in the smaller vessel category. Our main result is that nerve alignment lags vessel growth for these vessels, and, thus, the influence of any potential vessel shift can be assumed to be negligible.

In summary, Aim 1 shows that neurovascular alignment arises after microvascular network growth along arterioles, venules and even capillaries, and suggests that neurogenesis lags behind angiogenesis in the adult rat mesentery. Current research on neurovascular patterning focuses on determining the molecular cues and cell dynamics which lead to neurovascular alignment. The results from this study offers insight into when and where neurovascular alignment occurs during a time course of microvascular network growth. Defining the related functional interactions and mechanisms in the adult will have important implications for tissue engineering, regenerative medicine and neurodegenerative associated vascular diseases.

4.1.1 Limitations

The results of Aim 1 show that angiogenesis precedes neurovascular alignment in adult rat mesenteric windows. In order to fully generalize the findings, similar studies should be conducted in other models of angiogenesis, and in other species. The adult rat mesentery was used because it provides an *en face* view of microvascular and neural

networks in two dimensions. However, the function of the rat mesentery is unclear, raising questions of its relevance and applicability to other tissues. Additionally, all tissues are not two dimensional. The spatiotemporal distribution of neurovascular alignment across the microvascular hierarchy may deviate in three dimensional tissues. Identification of the nerves analyzed in the mesentery as sympathetic was confirmed by labeling for tyrosine hydroxylase. Various types of nerves are also present throughout the body, and may exhibit different growth dynamics and relationships with the microvasculature.

4.2 Identification of Class III β -Tubulin as a Marker of Angiogenic Pericytes and its Function in Human Brain Microvascular Pericytes

The primary findings of this study are that class III β -tubulin identifies a sub-population of perivascular cells, including pericytes and smooth muscle cells, and that class III β -tubulin is functionally involved in proliferation and migration of human pericytes. Class III β -tubulin coverage along vessels in growing rat mesenteric microvascular networks temporally and spatially correlates with capillary sprouting. Furthermore, inhibition of class III β -tubulin in human brain vascular pericytes reduced the fraction of proliferating cells and their migratory capability. The transient upregulation by perivascular cells and impairment of angiogenic processes caused by its suppression implicates class III β -tubulin as a functional marker of angiogenic pericytes and smooth muscle cells.

Vascular pericytes are critical players in angiogenesis and represent therapeutic targets [4,31]. Pericytes are functionally associated with regulating blood vessel permeability, vessel diameter, and endothelial cell proliferation [34,35]. Pericytes can also lead sprouting endothelial cells and even bridge the gaps between two sprouting segments [39,40]. Through cell-cell and cell-matrix interactions, pericytes are involved in contractile force transmission, vessel stabilization and endothelial cell survival. As such, pericytes have recently emerged as a cellular target to inhibit angiogenesis during tumor growth [41,42]. Though the full scope of intercellular signaling between pericytes and endothelial cells is still not well understood, work in this area has established that the pericyte-endothelial cell communication is governed by Ang-1/Tie2, TGF- β and PDGF-B/PDGFR- β interactions [38]. The next critical step to advancing pro- or anti-

angiogenic therapies will require the ability to identify specific populations of pericytes and their related dynamics. While common pericyte markers include SM α -actin, desmin, and PDGFR- β , their expression is not cell specific [4]. Their expressions often overlap and are distributed heterogeneously along the hierarchy of a network [48]. Our results suggest that class III β -tubulin could be used to delineate a perivascular cell sub-population only present during angiogenesis.

An emerging area of microvascular research focuses on the link between neural and vascular patterning [18,97]. This link is supported at the molecular level when considering growth inhibitors in the CNS such as ephrins, semaphorins, NG2, neuropilins (NPs) and Nogo [88]. In the vascular system, these molecules also appear to play regulatory roles in endothelial cell migration at the tips of capillary sprouts. All together a coordinated link between neural and vascular patterning is just beginning to be characterized and offers an exciting new perspective on the study of adult microvascular remodeling. Recently Neuron-glia antigen 2 (NG2), a marker of glial and neural progenitor cells in the central nervous system, was identified as a pericyte marker and as having a functional role in angiogenesis [11,39,53,54]. The common use of NG2 as a pericyte marker and its characterization raises the question of whether other neural phenotypic markers identify pericytes during angiogenesis. Similar to NG2, class III β -tubulin is considered a marker of neural progenitor cells in the CNS and peripheral nerves in the adult. In this study we demonstrate that class III β -tubulin is not nerve specific, and is transiently expressed by perivascular cells during network growth, providing another example of phenotypic commonality between neural and vascular systems.

Class III β -tubulin is one of seven β -tubulin isotypes which form α/β -tubulin heterodimers with six α -tubulin isotypes during the assembly of microtubules [57]. In the central nervous system, III β -tubulin is an early neuron-specific cytoskeletal marker during development, and has been associated with neuronal differentiation and neurogenesis [58]. Additionally, it is a cytoskeletal component in peripheral nerves and has been linked to prolonged cell cycling, cell survival, and cell migration [59,60]. Although class III β -tubulin expression is almost entirely specific to the nervous system in normal tissues, its expression in non-neuronal cancers correlates with resistance to tubulin-binding agents, high metastatic potential and malignancy [57,59,61,62]. Proteins associated with III β -tubulin expression are also involved in cellular responses to oxidative stress and glucose deprivation [63]. Typically, microtubules are associated with cell proliferation, motility and intracellular signaling [1]. Accordingly, we examined proliferation and migration of human pericytes after functional inhibition using siRNA. Our data suggests that class III β -tubulin in pericytes plays an important role in these two processes which are essential for normal angiogenesis [35,43]. Still, specific functions of class III β -tubulin are unclear and future studies will be required to elaborate on its mechanistic roles during angiogenesis *in vivo*.

Additional studies will also be required to confirm class III β -tubulin perivascular cell labeling in other tissues, and in response to additional angiogenic stimuli. The rat mesentery does represent a model to gain insight into the cellular phenotypes involved in angiogenesis [11,40]. It was selected because it allows two dimensional observations

across the entire hierarchy of an intact microvascular network down to the cellular and sub-cellular level. While our compound 48/80 injections stimulate angiogenesis by mast cell activation and histamine release, the exact triggering mechanisms are unclear [73,74]. It produces a robust response over a relatively short time course by mechanisms inherent to the angiogenic process. In support of our observation not being stimulation specific, class III β -tubulin upregulation by perivascular cells was observed along capillary sprouts in unstimulated tissues. Additionally, we confirmed our observations in angiogenic mesenteric networks stimulated by chronic hypoxia and tissue exteriorization (Figure 16). The chronic hypoxia model represents a more physiological stimulus and is relevant to tissue ischemia scenarios. The exteriorization model represents an alternative inflammatory stimulus.

During microvascular network growth, class III β -tubulin labeling transiently identified perivascular cells, including smooth muscle cells along larger sized vessels and pericytes along capillaries and post capillary venules. Labeling along blood vessels was perivascular cell specific and absent from blood endothelial cells. While all class III β -tubulin positive perivascular cells co-expressed NG2, not all NG2 positive cells expressed class III β -tubulin. In addition, only approximately 25% of capillary sprouts were covered with this cell type. This suggests that class III β -tubulin labeling identifies a subset of perivascular cells and emphasizes the need to understand the potential functional differences between class III β -tubulin positive and negative cell types.

To explore the functional role of class III β -tubulin in pericytes, we employed siRNA inhibition on human brain vascular pericytes (hBVPCs), and examined their proliferative and migratory behavior. Inhibition was confirmed by immunolabeling for class III β -tubulin 72 hours after transfection. Although we have not confirmed class III β -tubulin suppression at the RNA level for this study, immunolabeling was sufficient to show that siRNA achieved a reduction in class III β -tubulin expression in a subpopulation of cells when the assays were started. Additionally, immunolabeling after the assays were completed demonstrated that a class III β -tubulin expression remained suppressed in a population of pericytes throughout the assays. Future studies are necessary to quantify the RNA knockdown and its resultant protein knockdown, in order to optimize suppression of class III β -tubulin.

Class III β -tubulin suppression reduced the percentage of Ki67 positives hBVPCs by 10%. This implicates class III β -tubulin in either a functional role during cell proliferation, or associates it with a more viable cell type. In either case, expression of class III β -tubulin by pericytes during angiogenesis would be advantageous for increasing pericyte investment in newly formed vasculature. Ki67 is present in cells during all active segments of the cell cycle, but not in quiescent cells. Further studies should be aimed at elucidating the specific phases of the cell cycle and mechanisms of cell proliferation in which class III β -tubulin is involved.

Class III β -tubulin inhibition also effected migration into a scratch wound on confluent monolayers of hBVPCs. After 6 hours, scratch closure for class III β -tubulin-inhibited

cells was 20% less than cells transfected with Control siRNA. All scratches were similar areas prior to migration, and cell seeding numbers were matched prior to plating so that each sample contained similar cell densities during the assay. While the reduction in proliferation caused by class III β -tubulin inhibition may have attenuated scratch closure, the time course of 6 hours was not expected to be long enough for significant proliferation to take place. Additionally, cell densities at the end of the experiment remained similar. The results suggest that class III β -tubulin has a functional role in migration of hBVPCs. In accordance with the results, pericytes are thought to migrate along sprouting vasculature during angiogenesis [35,43]. Class III β -tubulin expression by angiogenic pericytes may indicate a migratory phenotype, although *in vivo* studies are necessary for confirmation.

Expression of class III β -tubulin by non-neuronal tumors correlates with their resistance to tubulin binding drugs such as paclitaxel [58,62]. Class III β -tubulin inhibition sensitizes cancer cells to paclitaxel treatment. Inhibiting class III β -tubulin does not affect proliferation or migration in the absence of paclitaxel. However, treatment with the drug in the absence of class III β -tubulin expression decreases their proliferative and migratory capabilities compared to cells expressing the tubulin [59,61,62]. Accordingly, paclitaxel treatment was used to investigate whether class III β -tubulin rendered hBVPCs resistant to such drugs. Our results show that paclitaxel treatment inhibited the migration response of all groups. Although the percent change in scratch closure was -40% between the paclitaxel-treated Control siRNA and Target siRNA compared to -22% between the untreated groups, the Sham and Control siRNA groups also exhibited similar percent

changes between untreated and treated groups. This suggests that transfection may amplify the effects of paclitaxel treatment. Future studies should aim to reduce variability between the Sham and transfected samples by decreasing transfection time. Further analysis can be performed to determine cell-specific trends within the target siRNA group. The migratory and proliferative capabilities of class III β -tubulin-positive and -negative cells can be assessed cell-by-cell and compared between the untreated and paclitaxel-treated samples. Additionally, hBVPC responses to varying doses during proliferation and migration should be assessed to determine whether class III β -tubulin resistance saturates with different drug concentrations.

In summary, this study identifies class III β -tubulin as a new pericyte marker that is only expressed along remodeling vessels involved in angiogenesis. While characterization of class III β -tubulin in other angiogenic scenarios and species are required to fully generalize our findings, our results suggest that class III β -tubulin can be used for the identification of a specific perivascular cell population involved in angiogenesis. They also suggest that class III β -tubulin may play a mechanistic role in proliferation and migration of pericytes during angiogenesis, although further validation *in vivo* is required to fully substantiate our findings.

4.2.1 Limitations

The results of Aim 2 show that class III β -tubulin is transiently expressed by perivascular cells during angiogenesis in the adult rat mesentery. Although the expression of class III β -tubulin by human-derived pericytes was confirmed *in vitro*, its expression by human

pericytes during angiogenic scenarios *in vivo* in human tissue has not been confirmed.

The results also suggest that class III β -tubulin expression plays a role in human pericyte proliferation and migration. However, these results have not yet been confirmed *in vivo* either. Demonstrating that inhibition of class III β -tubulin reduces proliferation and migration during angiogenesis would significantly support our conclusions.

4.3 An Angiogenesis Model for Investigating Multicellular Interactions across Intact Microvascular Networks

This study establishes the rat mesentery culture model as a tissue culture system that enables investigators to study adult microvascular growth and remodeling within an intact microvascular network. The rat mesentery culture model is advantageous because it 1) contains the hierarchy of microvessels including arterioles, venules, and capillaries; 2) contains endothelial cells, smooth muscle cells and pericytes; and 3) can be used to probe mechanistic cell-cell interactions at specific locations within a microvascular network during angiogenesis.

The rat mesentery has been previously cultured to examine proliferation and cytochemical activity of fibroblasts and mesothelial cells during wound healing [98]. During culture mast cells, blood vessels and lymphatic vessels remained intact [98]. In the current study, we show that cultured mesenteric microvascular networks can be stimulated to undergo angiogenesis. An advantage of the rat mesentery culture model is that angiogenesis can be evaluated at different locations within an intact microvascular network. Another *ex vivo* model that offers this capability is the retinal explant assay. However, for the retinal explant assay, the ability to investigate either pericyte-endothelial or blood endothelial-lymphatic endothelial cell interactions has not been demonstrated. The serum free media culture conditions used in the current study are similar to those used for the aortic ring assay, [68] and are sufficient to keep resident cells alive during endothelial sprouting. The culture conditions allowed the vasculature to maintain typical arterial/venous identities and endothelial cell, smooth muscle cell and

pericyte morphologies observed *in vivo* [11,78,99]. Compared to the aortic ring and retinal explant assays, an advantage of our culture method is its simplicity. In the rat mesentery culture model, tissues can be allowed to freely float in media while in culture and require minimal preparation. Since vessel growth occurs within the intact tissue, the model system is self-contained and does not require embedding into a matrix. Similar to the aortic ring and retinal explant assays, the supplement of growth factors served to increase capillary sprouting in the mesentery culture model [100-102].

In other *ex vivo* models, angiogenesis is evaluated on an avascular background, resulting in essentially binary angiogenic responses compared to controls. For example, bFGF supplemented media (identical concentration as our model) induced approximately a 275 % increase compared to controls in the aortic ring assay over 7 days [71]. In our model, bFGF supplemented media resulted in a 99% increase in capillary sprouting off of venules and a 41% increase in capillary sprouting off of capillaries. While the nominal angiogenic effect in our study is less, it is more in line with the *in vivo* response percentages for rat mesenteric microvascular networks stimulated by i.p. injections of bFGF [76]. These comparisons suggest that cultured rat mesentery responses might be more comparable to *in vivo* responses rather than those reported for other *ex vivo* models. The rat mesentery culture model is also characterized by a high variation in responses. The combination of smaller nominal changes and variation in responses suggests that the statistical considerations made for *in vivo* experiments should also be made for with the rat mesentery culture model.

In addition, we show that cultured mesentery tissues contain initial lymphatic networks that maintain their branching architecture and LYVE-1 lymphatic marker identity.

Nerves are also present and label positively for class III β -tubulin, which is an established nerve marker in this tissue type [80]. A critical issue for the use of the rat mesentery culture model is cell differentiation and function. Three days was selected for our study because at this time point we confirmed NG2 arterial/venous differentiation, the presence of NG2 positive pericytes along capillaries, and the presence of intact lymphatic networks. By 7 days, the number of NG2 positive perivascular cells is reduced. These qualitative observations at 7 days motivate future studies to evaluate the maintenance of specific cell phenotype and function.

Capillary sprouting in bFGF stimulated networks preferentially occurred from capillaries and venules rather than from arterioles. The spatial location of sprouts within a microvascular network is consistent with *in vivo* observations [3]. bFGF and VEGF have been previously documented as potent angiogenic stimulators [76,100]. We show that both growth factors are capable of inducing capillary sprouting in the rat mesentery culture model. It should be noted that the MEM alone control groups for each growth factor experiment were not the same. This difference highlights the potential for results to be dependent on network heterogeneity commonly observed in different rat littermates. For the respective growth factor experiments, tissues were harvested from the same littermates. We also show that both bFGF- and VEGF-stimulated angiogenesis can be inhibited by targeting NG2 positive pericytes. For the growth factor and inhibition studies, media was changed every 2 days to replenish the supply of supplement. While

our results do show that changes every 2 days are sufficient, future experiments will be needed to compare whether replenishing the supplement daily versus every 2 days influences the tissue response.

Our observation of a VEGF specific increase in apparent lymphatic/blood endothelial cell connections serves an example of using the rat mesentery culture model for investigating interrelationships between lymphatic and blood vessel systems. Our results suggest that connections across systems are dynamic and can be influenced by the local environment. In our laboratory's original characterization of these connections in unstimulated adult rat mesenteric networks, connections were shown to be non-luminal. The lack of perfusion in the culture model limits the ability to evaluate whether the connections stimulated by VEGF become functional. Still, the observations of apparent interactions between lymphatic and blood endothelial cells supports the potential for the rat mesentery culture model to be used for future studies aimed at understanding how angiogenesis and lymphangiogenesis are related. Recently, a lymphatic analog to the aortic ring assay was introduced as a tool for identifying lymphatic molecular mechanisms *in vitro* [103]. In contrast to both lymphatic and aortic ring assays, the rat mesentery culture model enables simultaneous investigation of both systems along intact networks.

Elaboration on the rat mesentery culture model allowed imaging from the same network before and after 20% serum stimulation demonstrating 1) the use of the model for cell tracking experiments and 2) the ability for vascular islands to connect to a nearby, growing network [104]. Twenty percent serum was selected as the stimulus because it

produces a dramatic increase in vessel density (i.e. the formation of new vessel segments) indicative of network growth as compared to the growth factor stimulations. Over the 3 day culture time course, both bFGF and VEGF caused an increase in capillary sprouting, but not necessarily an increase in the vessel density. Comparison of BSI-lectin labeled networks before and after angiogenesis identified new vessel formation and the fate of initially disconnected endothelial cell segments, termed vascular islands. The utility of the model allowed us to show that vascular islands can connect to nearby growing vascular networks. This result confirms a novel cellular dynamic involved in angiogenesis and demonstrates the potential for this model to be used for time lapse observation of single cell dynamics [104].

Characterization of rat mesenteric tissues chronically stimulated to undergo angiogenesis *in vivo* has proven valuable for identifying cellular dynamics during capillary sprout formation [75,105]. The rat mesentery tissue is 20 μm – 40 μm thick and offers an *en face* view of intact microvascular networks down to the single cell level [106]. In the current study, we demonstrate that this tissue can be cultured and stimulated to undergo angiogenesis over a 3 day time course. Compared to chronic *in vivo* experiments, our model allows for investigation of multiple angiogenic scenarios and real time imaging in the same tissue, within a controllable environment free of systemic side effects.

A current limitation of this model is that we do not know how long the microvascular network structure can be maintained in culture. However, we do show that structure can be maintained for at least 3 days, a duration sufficient for the induction of angiogenesis.

Another limitation is that the rat mesentery culture model lacks the presence of blood flow and related shear stresses, which have been implicated in the regulation and guidance of angiogenesis [65,105,107]. The absence of shear stress is similarly a limitation of common *in vitro* and *ex vivo* culture assays such as 2D endothelial cell cultures, 3D matrix systems and the aortic ring assay; all of which have been proven extremely valuable for studying angiogenesis [64,68,108]. The model also requires rat mesenteric connective tissue eliminating the potential use of murine-derived mesenteric tissues derived from knock out animals. Unfortunately, based on our experience and reports from others, the same connective tissue in the mouse is mostly avascular [106]. The question whether growth can be stimulated in mouse mesenteric windows remains and requires future trials with different mouse strains and stimuli. Anghelina et al. reports the ability of i.p. injections of VEGF and mechanical irritation to stimulate capillary ingrowth into otherwise avascular mesenteric windows [109].

In conclusion, the rat mesentery culture model offers an innovative tool for investigating angiogenesis. It provides an assay for observing cell dynamics involved in capillary sprouting at specific locations within a microvascular network and for functional studies in an intact tissue. Use of the rat mesentery culture model could provide valuable insight into the cellular interactions involved in angiogenesis and motivates a new line of experiments aimed at understanding the interrelationships between angiogenesis, lymphangiogenesis and neurogenesis.

4.3.1 Limitations

The results of Aim 3 indicate that the rat mesentery culture model can be used to study multicellular interactions during angiogenesis as demonstrated by stimulation of capillary sprouting using angiogenic factors, and manipulation of capillary sprouting by targeting pericytes. However, when the tissue is cultured, blood flow has been removed from the system. This is a major drawback to many current tissue explant models including the aortic ring assay because flow mediates endothelial cells dynamics. Another limitation of the mesentery culture model is that transgenic rat models are difficult to develop. The mesentery culture model would be much more powerful with the capability of genetic manipulation for cell lineage studies and mechanistic inhibition.

CHAPTER 5: CONCLUSIONS

The overall objectives of this study were to identify links between the microvasculature and nervous system during angiogenesis in the adult, and establish a model to probe specific cellular and molecular interactions within intact microvascular networks and across systems in a controlled environment. To complete these objectives, we aimed to 1) determine the spatiotemporal relationship between angiogenesis and neurovascular alignment; 2) determine whether class III β -tubulin is a functional marker of perivascular cells during angiogenesis; and 3) develop an *in vitro* culture model using the adult rat mesentery to investigate multicellular and multisystem interactions during angiogenesis within intact microvascular networks.

We observed that sympathetic neural alignment with the microvasculature occurs across all vessel types in adult rat mesentery microvascular networks after angiogenesis has subsided. The results suggest that nerves are not necessary for angiogenesis, but may play a role in vessel maturation after network expansion has occurred. In addition, this study highlights that the anatomical neurovascular link persists through adulthood down to the capillary level.

Analysis of the neural marker class III β -tubulin in Aim 1 revealed that it is transiently expressed by perivascular cells in microvascular networks, including pericytes and

smooth muscle cells, during angiogenesis. Expression of class III β -tubulin by vascular cells emphasizes another shared phenotypic link between the vascular and neural systems. The results suggest that class III β -tubulin expression represents a subset of perivascular cells which are active during angiogenesis. Furthermore, class III β -tubulin may play a functional role in human brain vascular pericyte proliferation and migration - two important processes during angiogenesis.

The importance of class III β -tubulin expression during angiogenesis remains unclear because current experimental methods to investigate pericyte-endothelial cell interactions are limited by insufficient spatial resolution, unknown delivery efficacy and lack of local environmental control. The rat mesentery culture model was established to examine such microvascular dynamics and the relationships among systems across intact networks in a controlled environment. It is a new tool to study multicellular and multisystem interactions during microvascular growth. Our results show that the model contains the hierarchy of microvessels including arterioles, venules, and capillaries; contains endothelial cells, smooth muscle cells and pericytes; can be used to probe mechanistic cell-cell interactions at specific locations within a microvascular network during angiogenesis; can be used to investigate the interrelationships between angiogenesis, lymphangiogenesis and neurogenesis; and can be used to track the fate of cellular structures during microvascular network remodeling.

CHAPTER 6: FUTURE STUDIES

In Aim 1, we showed that neurovascular alignment is not necessary for angiogenesis in the adult. The role that nerves play in later microvascular remodeling events such as arteriogenesis remains under-investigated. Whether nerves influence arterial/venous identity after angiogenesis, or vessel identity participates in neural guidance also remains unclear. We established class III β -tubulin as a marker of angiogenic perivascular cells and indicate its function in pericytes during angiogenesis in Aim 2. However, class III β -tubulin expression by pericytes has not been characterized in all tissues or angiogenic scenarios, and its function *in vivo* has not been confirmed. Whether class III β -tubulin represents a valid target to manipulate angiogenesis also remains to be investigated. Aim 3 established the rat mesentery culture model as a tool to investigate multicellular and multisystem interactions during angiogenesis within intact microvascular networks. The new model can now be used to determine whether class III β -tubulin expression by pericytes effects angiogenesis. Additionally, the model's full utility in tracing cell lineage and testing pro- and anti-angiogenic factors has not been fully explored.

6.1 Spatiotemporal Relationship between Angiogenesis and Neurovascular

Alignment

Our results showed that neurovascular alignment occurs across the entire microvascular hierarchy, and suggest that nerves are not necessary for angiogenesis. However, nerves may play a role in vessel maturation after network expansion has occurred. These findings motivate studies aimed at determining whether neural function is necessary for neurovascular alignment or microvascular remodeling. Using sympathetic neurotransmitter blockers, neural function will be blocked during angiogenesis by i.p. injection or micro-osmotic pump. Neurovascular alignment and angiogenesis will be quantified. However, because neural function influences microvascular function, results may reflect secondary effects of impairment on the microcirculation.

Whether neurovascular alignment correlates with vessel maturation and arterial-venous identity selection, or a lack of neurovascular alignment correlates with vessel regression remains to be determined. Vessels can be labeled with smooth muscle α -actin, and the proportion of smooth muscle α -actin positive vessels aligned with nerves can be quantified to indicate vessel maturation. Using arterial and venous specific endothelial cell markers, vessel identities of aligned and non-aligned capillaries over the time course of angiogenesis can be quantified to suggest whether the fate of capillaries is affected by neurovascular alignment. To determine whether neurovascular alignment can prevent regression, we can extend our harvesting time point out to 70 days when networks are regressing [110], and compare neurovascular alignment between fully vascularized and regressing networks. This study will require analysis of neural density pre- and post-

regression as well. Correlation between neurovascular alignment and vessel maturation, identity fate or regression would suggest a neural signal influencing vascular remodeling.

The next studies would focus on elucidating those signals.

6.2 Class III β -Tubulin as a Functional Marker of Perivascular Cells during Angiogenesis

Our results identify class III β -tubulin as a new pericyte marker that is expressed by a population of cells involved in angiogenesis. However, characterization of class III β -tubulin in other angiogenic scenarios and species is required to fully generalize our findings. Various *in vivo* models of angiogenesis should be used to determine whether class III β -tubulin is expressed by pericytes in all angiogenic scenarios, or a subset. For example, sections of human, rat and mouse tumors which are highly angiogenic should be immunolabeled for class III β -tubulin and pericyte markers to substantiate our findings in a pathological scenario. Phenotypic heterogeneity in pericyte populations across the microvascular hierarchy still raises questions about their varying functions in angiogenesis versus stabilization. Characterizing pericyte the overlapping expression of class III β -tubulin with other pericyte markers, such as NG2 and PDGFR β may lead to a better understanding of different pericyte subpopulations.

Our results also suggest that class III β -tubulin may play a mechanistic role in proliferation and migration of pericytes during angiogenesis. These functions must be confirmed *in vivo* or *in situ*. Using the *in vivo* angiogenesis models or the rat mesentery culture model, loss-of-function studies can indicate whether it is important for microvascular remodeling. Quantifying angiogenesis in a normal versus class III β -tubulin-inhibited mesentery cultures can indicate whether class III β -tubulin function is necessary for angiogenesis. To determine its role in pericyte migration and proliferation, pericyte coverage across the hierarchy of microvascular networks could be quantified

over the time course of angiogenesis *in vivo* after inhibition. Additionally, proliferation markers such as BrdU and Ki67 can be used to indicate whether loss of class III β -tubulin correlates with impaired perivascular cell proliferation.

Since pericyte-endothelial cell interactions are critical for angiogenesis, investigating the role of class III β -tubulin function in pericyte-endothelial cell interactions may be important. *In vitro* co-culture models of endothelial cells and pericytes embedded in matrix protein has been used to study tubulogenesis and basement membrane deposition [46]. The importance of class III β -tubulin in pericyte-endothelial cell interactions can be analyzed by quantifying vascular tube density, pericyte investment and basement membrane deposition. Additionally, endothelial cell proliferation should be quantified to determine whether inhibiting class III β -tubulin interferes with pericyte regulation of endothelial cell function.

6.3 The Adult Rat Mesentery as a Model for Multicellular and Multisystem

Interactions during Angiogenesis

Our results from Aim 3 establish the rat mesentery culture model for investigating multicellular and multisystem interactions. Future studies should use the model to improve our understanding of pericyte-endothelial cell interactions during angiogenesis, and the growth relationships between the vascular and lymphatic systems. For example, quantifying capillary sprouting in the rat mesentery culture model after inhibition of class III β -tubulin using siRNA would provide valuable insight to its necessity in pericytes during angiogenesis and for pericyte-endothelial cell interactions. While use of siRNA in the model has not yet been validated, the *in vitro* setting allows for the desired control over the culture environment for successful transfection.

Although nerves were shown to be present in the culture model, their function and viability for studies on neurovascular interactions are questionable. Establishing the rat mesentery culture model for studying neurogenesis would allow studies focused on neurovascular signaling during angiogenesis and vessel maturation. To further expand the capability of the model, studies should aim to incorporate outside cellular components to investigate the role of exogenous stem cells in angiogenesis, or dynamics of angiogenesis and lymphangiogenesis in response to tumor progression.

One of the central drawbacks to the system is that flow is not present in the culture model. Canulation of microvessels in culture to establish flow through networks would significantly improve the physiological relevance of the rat mesentery culture model. An

additional improvement to the model would be the ability to genetically manipulate specific targets. Since transgenic rats are difficult to breed, the rat mesentery culture model may have limited applications. However, considering the potential applications, culturing the mesentery of transgenic mice is worth exploring despite its documented lack of microvasculature.

7. REFERENCES

- [1] Boron WF, Boulpaep EL: Medical Physiology,ed Updated Edition. Elsevier Saunders, Philidelphia, Pennsylvania, 2005.
- [2] Fung YC: Microcirculation; Biomechanics: Circulation. Springer Science+Busness Media, LLC, New York, New York, 1997, pp 266-332.
- [3] Rhodin JA, Fujita H: Capillary growth in the mesentery of normal young rats. Intravital video and electron microscope analyses, J Submicrosc Cytol Pathol. 1989;21:1-34.
- [4] Gerhardt H, Betsholtz C: Endothelial-pericyte interactions in angiogenesis, Cell Tissue Res. 2003;314:15-23.
- [5] Shepro D, Morel NM: Pericyte physiology, FASEB J. 1993;7:1031-1038.
- [6] Fukumura D, Jain RK: Tumor microvasculature and microenvironment: targets for anti-angiogenesis and normalization, Microvasc Res. 2007;74:72-84.
- [7] Peirce SM, Skalak TC: Microvascular remodeling: a complex continuum spanning angiogenesis to arteriogenesis, Microcirculation. 2003;10:99-111.
- [8] Folkman J: Seminars in Medicine of the Beth Israel Hospital, Boston. Clinical applications of research on angiogenesis, N Engl J Med. 1995;333:1757-1763.
- [9] Carmeliet P: Angiogenesis in life, disease and medicine, Nature. 2005;438:932-936.
- [10] Ferrara N: Role of vascular endothelial growth factor in regulation of physiological angiogenesis, Am J Physiol Cell Physiol. 2001;280:C1358-66.
- [11] Murfee WL, Rehorn MR, Peirce SM, Skalak TC: Perivascular cells along venules upregulate NG2 expression during microvascular remodeling, Microcirculation. 2006;13:261-273.
- [12] Carmeliet P, Tessier-Lavigne M: Common mechanisms of nerve and blood vessel wiring, Nature. 2005;436:193-200.

- [13] Gerhardt H, Golding M, Fruttiger M, Ruhrberg C, Lundkvist A, Abramsson A, Jeltsch M, Mitchell C, Alitalo K, Shima D, Betsholtz C: VEGF guides angiogenic sprouting utilizing endothelial tip cell filopodia, *J Cell Biol.* 2003;161:1163-1177.
- [14] Mukoyama YS, Shin D, Britsch S, Taniguchi M, Anderson DJ: Sensory nerves determine the pattern of arterial differentiation and blood vessel branching in the skin, *Cell.* 2002;109:693-705.
- [15] Gerhardt H: VEGF and endothelial guidance in angiogenic sprouting, *Organogenesis.* 2008;4:241-246.
- [16] Armulik A, Abramsson A, Betsholtz C: Endothelial/pericyte interactions, *Circ Res.* 2005;97:512-523.
- [17] Segal SS: Regulation of blood flow in the microcirculation, *Microcirculation.* 2005;12:33-45.
- [18] Weinstein BM: Vessels and nerves: marching to the same tune, *Cell.* 2005;120:299-302.
- [19] Larrivee B, Freitas C, Suchting S, Brunet I, Eichmann A: Guidance of vascular development: lessons from the nervous system, *Circ Res.* 2009;104:428-441.
- [20] Ponnambalam S, Alberghina M: Evolution of the VEGF-regulated vascular network from a neural guidance system, *Mol Neurobiol.* 2011;43:192-206.
- [21] Tam SJ, Watts RJ: Connecting vascular and nervous system development: angiogenesis and the blood-brain barrier, *Annu Rev Neurosci.* 2010;33:379-408.
- [22] Park JA, Choi KS, Kim SY, Kim KW: Coordinated interaction of the vascular and nervous systems: from molecule- to cell-based approaches, *Biochem Biophys Res Commun.* 2003;311:247-253.
- [23] Bates D, Taylor GI, Newgreen DF: The pattern of neurovascular development in the forelimb of the quail embryo, *Dev Biol.* 2002;249:300-320.
- [24] Bates D, Taylor GI, Minichiello J, Farlie P, Cichowitz A, Watson N, Klagsbrun M, Mamluk R, Newgreen DF: Neurovascular congruence results from a shared patterning mechanism that utilizes Semaphorin3A and Neuropilin-1, *Dev Biol.* 2003;255:77-98.
- [25] Martin P, Lewis J: Origins of the neurovascular bundle: interactions between developing nerves and blood vessels in embryonic chick skin, *Int J Dev Biol.* 1989;33:379-387.

- [26] Ogunshola OO, Stewart WB, Mihalcik V, Solli T, Madri JA, Ment LR: Neuronal VEGF expression correlates with angiogenesis in postnatal developing rat brain, *Brain Res Dev Brain Res*. 2000;119:139-153.
- [27] Ogunshola OO, Antic A, Donoghue MJ, Fan SY, Kim H, Stewart WB, Madri JA, Ment LR: Paracrine and autocrine functions of neuronal vascular endothelial growth factor (VEGF) in the central nervous system, *J Biol Chem*. 2002;277:11410-11415.
- [28] Mukoyama YS, Gerber HP, Ferrara N, Gu C, Anderson DJ: Peripheral nerve-derived VEGF promotes arterial differentiation via neuropilin 1-mediated positive feedback, *Development*. 2005;132:941-952.
- [29] Ferretti A, Boschi E, Stefani A, Spiga S, Romanelli M, Lemmi M, Giovannetti A, Longoni B, Mosca F: Angiogenesis and nerve regeneration in a model of human skin equivalent transplant, *Life Sci*. 2003;73:1985-1994.
- [30] Hobson MI, Brown R, Green CJ, Terenghi G: Inter-relationships between angiogenesis and nerve regeneration: a histochemical study, *Br J Plast Surg*. 1997;50:125-131.
- [31] Hirschi KK, D'Amore PA: Pericytes in the microvasculature, *Cardiovasc Res*. 1996;32:687-698.
- [32] Tilton RG, Kilo C, Williamson JR: Pericyte-endothelial relationships in cardiac and skeletal muscle capillaries, *Microvasc Res*. 1979;18:325-335.
- [33] Peppiatt CM, Howarth C, Mobbs P, Attwell D: Bidirectional control of CNS capillary diameter by pericytes, *Nature*. 2006;443:700-704.
- [34] Hellstrom M, Gerhardt H, Kalen M, Li X, Eriksson U, Wolburg H, Betsholtz C: Lack of pericytes leads to endothelial hyperplasia and abnormal vascular morphogenesis, *J Cell Biol*. 2001;153:543-553.
- [35] Lindahl P, Johansson BR, Leveen P, Betsholtz C: Pericyte loss and microaneurysm formation in PDGF-B-deficient mice, *Science*. 1997;277:242-245.
- [36] Suri C, Jones PF, Patan S, Bartunkova S, Maisonpierre PC, Davis S, Sato TN, Yancopoulos GD: Requisite role of angiopoietin-1, a ligand for the TIE2 receptor, during embryonic angiogenesis, *Cell*. 1996;87:1171-1180.
- [37] Uemura A, Ogawa M, Hirashima M, Fujiwara T, Koyama S, Takagi H, Honda Y, Wiegand SJ, Yancopoulos GD, Nishikawa S: Recombinant angiopoietin-1 restores higher-order architecture of growing blood vessels in mice in the absence of mural cells, *J Clin Invest*. 2002;110:1619-1628.

- [38] Folkman J, D'Amore PA: Blood vessel formation: what is its molecular basis? *Cell*. 1996;87:1153-1155.
- [39] Ozerdem U, Monosov E, Stallcup WB: NG2 proteoglycan expression by pericytes in pathological microvasculature, *Microvasc Res*. 2002;63:129-134.
- [40] Ponce AM, Price RJ: Angiogenic stimulus determines the positioning of pericytes within capillary sprouts in vivo, *Microvasc Res*. 2003;65:45-48.
- [41] Ozerdem U: Targeting of pericytes diminishes neovascularization and lymphangiogenesis in prostate cancer, *Prostate*. 2006;66:294-304.
- [42] Song S, Ewald AJ, Stallcup W, Werb Z, Bergers G: PDGFRbeta+ perivascular progenitor cells in tumours regulate pericyte differentiation and vascular survival, *Nat Cell Biol*. 2005;7:870-879.
- [43] Hellstrom M, Kalen M, Lindahl P, Abramsson A, Betsholtz C: Role of PDGF-B and PDGFR-beta in recruitment of vascular smooth muscle cells and pericytes during embryonic blood vessel formation in the mouse, *Development*. 1999;126:3047-3055.
- [44] Lindblom P, Gerhardt H, Liebner S, Abramsson A, Enge M, Hellstrom M, Backstrom G, Fredriksson S, Landegren U, Nystrom HC, Bergstrom G, Dejana E, Ostman A, Lindahl P, Betsholtz C: Endothelial PDGF-B retention is required for proper investment of pericytes in the microvessel wall, *Genes Dev*. 2003;17:1835-1840.
- [45] Hammes HP, Lin J, Renner O, Shani M, Lundqvist A, Betsholtz C, Brownlee M, Deutsch U: Pericytes and the pathogenesis of diabetic retinopathy, *Diabetes*. 2002;51:3107-3112.
- [46] Stratman AN, Malotte KM, Mahan RD, Davis MJ, Davis GE: Pericyte recruitment during vasculogenic tube assembly stimulates endothelial basement membrane matrix formation, *Blood*. 2009;114:5091-5101.
- [47] Saunders WB, Bohnsack BL, Faske JB, Anthis NJ, Bayless KJ, Hirschi KK, Davis GE: Coregulation of vascular tube stabilization by endothelial cell TIMP-2 and pericyte TIMP-3, *J Cell Biol*. 2006;175:179-191.
- [48] Nehls V, Drenckhahn D: The versatility of microvascular pericytes: from mesenchyme to smooth muscle? *Histochemistry*. 1993;99:1-12.
- [49] Siczekiewicz GJ, Herman IM: TGF-beta 1 signaling controls retinal pericyte contractile protein expression, *Microvasc Res*. 2003;66:190-196.
- [50] Doherty MJ, Ashton BA, Walsh S, Beresford JN, Grant ME, Canfield AE: Vascular pericytes express osteogenic potential in vitro and in vivo, *J Bone Miner Res*. 1998;13:828-838.

- [51] Balabanov R, Washington R, Wagnerova J, Dore-Duffy P: CNS microvascular pericytes express macrophage-like function, cell surface integrin alpha M, and macrophage marker ED-2, *Microvasc Res.* 1996;52:127-142.
- [52] Dore-Duffy P, Katychew A, Wang X, Van Buren E: CNS microvascular pericytes exhibit multipotential stem cell activity, *J Cereb Blood Flow Metab.* 2006;26:613-624.
- [53] Ozerdem U, Grako KA, Dahlin-Huppe K, Monosov E, Stallcup WB: NG2 proteoglycan is expressed exclusively by mural cells during vascular morphogenesis, *Dev Dyn.* 2001;222:218-227.
- [54] Murfee WL, Skalak TC, Peirce SM: Differential arterial/venous expression of NG2 proteoglycan in perivascular cells along microvessels: identifying a venule-specific phenotype, *Microcirculation.* 2005;12:151-160.
- [55] Ozerdem U, Stallcup WB: Pathological angiogenesis is reduced by targeting pericytes via the NG2 proteoglycan, *Angiogenesis.* 2004;7:269-276.
- [56] Draberova E, Del Valle L, Gordon J, Markova V, Smejkalova B, Bertrand L, de Chadarevian JP, Agamanolis DP, Legido A, Khalili K, Draber P, Katsetos CD: Class III beta-tubulin is constitutively coexpressed with glial fibrillary acidic protein and nestin in midgestational human fetal astrocytes: implications for phenotypic identity, *J Neuropathol Exp Neurol.* 2008;67:341-354.
- [57] Katsetos CD, Legido A, Perentes E, Mork SJ: Class III beta-tubulin isotype: a key cytoskeletal protein at the crossroads of developmental neurobiology and tumor neuropathology, *J Child Neurol.* 2003;18:851-66; discussion 867.
- [58] Katsetos CD, Herman MM, Mork SJ: Class III beta-tubulin in human development and cancer, *Cell Motil Cytoskeleton.* 2003;55:77-96.
- [59] Gan PP, McCarroll JA, Po'uha ST, Kamath K, Jordan MA, Kavallaris M: Microtubule dynamics, mitotic arrest, and apoptosis: drug-induced differential effects of betaIII-tubulin, *Mol Cancer Ther.* 2010;9:1339-1348.
- [60] Tischfield MA, Baris HN, Wu C, Rudolph G, Van Maldergem L, He W, Chan WM, Andrews C, Demer JL, Robertson RL, Mackey DA, Ruddle JB, Bird TD, Gottlob I, Pieh C, Traboulsi EI, Pomeroy SL, Hunter DG, Soul JS, Newlin A, Sabol LJ, Doherty EJ, de Uzategui CE, de Uzategui N, Collins ML, Sener EC, Wabbels B, Hellebrand H, Meitinger T, de Berardinis T, Magli A, Schiavi C, Pastore-Trossello M, Koc F, Wong AM, Levin AV, Geraghty MT, Descartes M, Flaherty M, Jamieson RV, Moller HU, Meuthen I, Callen DF, Kerwin J, Lindsay S, Meindl A, Gupta ML, Jr, Pellman D, Engle EC: Human TUBB3 mutations perturb microtubule dynamics, kinesin interactions, and axon guidance, *Cell.* 2010;140:74-87.

- [61] Gan PP, Pasquier E, Kavallaris M: Class III beta-tubulin mediates sensitivity to chemotherapeutic drugs in non small cell lung cancer, *Cancer Res.* 2007;67:9356-9363.
- [62] McCarroll JA, Gan PP, Liu M, Kavallaris M: betaIII-tubulin is a multifunctional protein involved in drug sensitivity and tumorigenesis in non-small cell lung cancer, *Cancer Res.* 2010;70:4995-5003.
- [63] Cicchillitti L, Penci R, Di Michele M, Filippetti F, Rotilio D, Donati MB, Scambia G, Ferlini C: Proteomic characterization of cytoskeletal and mitochondrial class III beta-tubulin, *Mol Cancer Ther.* 2008;7:2070-2079.
- [64] Goodwin AM: In vitro assays of angiogenesis for assessment of angiogenic and anti-angiogenic agents, *Microvasc Res.* 2007;74:172-183.
- [65] Kaunas R, Kang H, Bayless KJ: Synergistic Regulation of Angiogenic Sprouting by Biochemical Factors and Wall Shear Stress, *Cell Mol Bioeng.* 2011;4:547-559.
- [66] Koh W, Stratman AN, Sacharidou A, Davis GE: In vitro three dimensional collagen matrix models of endothelial lumen formation during vasculogenesis and angiogenesis, *Methods Enzymol.* 2008;443:83-101.
- [67] Staton CA, Reed MW, Brown NJ: A critical analysis of current in vitro and in vivo angiogenesis assays, *Int J Exp Pathol.* 2009;90:195-221.
- [68] Nicosia RF, Ottinetti A: Growth of microvessels in serum-free matrix culture of rat aorta. A quantitative assay of angiogenesis in vitro, *Lab Invest.* 1990;63:115-122.
- [69] Nicosia RF, Bonanno E, Villaschi S: Large-vessel endothelium switches to a microvascular phenotype during angiogenesis in collagen gel culture of rat aorta, *Atherosclerosis.* 1992;95:191-199.
- [70] Nicosia RF, Villaschi S: Rat aortic smooth muscle cells become pericytes during angiogenesis in vitro, *Lab Invest.* 1995;73:658-666.
- [71] Villaschi S, Nicosia RF: Angiogenic role of endogenous basic fibroblast growth factor released by rat aorta after injury, *Am J Pathol.* 1993;143:181-190.
- [72] Norrby K, Jakobsson A, Sorbo J: Quantitative angiogenesis in spreads of intact rat mesenteric windows, *Microvasc Res.* 1990;39:341-348.
- [73] Norrby K, Jakobsson A, Sorbo J: Mast-cell-mediated angiogenesis: a novel experimental model using the rat mesentery, *Virchows Arch B Cell Pathol Incl Mol Pathol.* 1986;52:195-206.

- [74] Franzen L, Ghassemifar R, Malcherek P: Experimental mast cell activation improves connective tissue repair in the perforated rat mesentery, *Agents Actions*. 1991;33:371-377.
- [75] Stapor PC, Murfee WL: Identification of class III beta-tubulin as a marker of angiogenic perivascular cells, *Microvasc Res*. 2011.
- [76] Norrby K: Basic fibroblast growth factor and de novo mammalian angiogenesis, *Microvasc Res*. 1994;48:96-113.
- [77] Norrby K: Vascular endothelial growth factor and de novo mammalian angiogenesis, *Microvasc Res*. 1996;51:153-163.
- [78] Yang M, Stapor PC, Peirce SM, Betancourt AM, Murfee WL: Rat mesentery exteriorization: a model for investigating the cellular dynamics involved in angiogenesis, *J Vis Exp*. 2012;(63). pii: 3954. doi:10.3791/3954.
- [79] Robichaux JL, Tanno E, Rappleye JW, Ceballos M, Stallcup WB, Schmid-Schonbein GW, Murfee WL: Lymphatic/Blood endothelial cell connections at the capillary level in adult rat mesentery, *Anat Rec (Hoboken)*. 2010;293:1629-1638.
- [80] Stapor PC, Murfee WL: Spatiotemporal Distribution of Neurovascular Alignment in Remodeling Adult Rat Mesentery Microvascular Networks, *J Vasc Res*. 2012;49:299-308.
- [81] Kelly-Goss MR, Winterer ER, Stapor PC, Yang M, Sweat RS, Stallcup WB, Schmid-Schonbein GW, Murfee WL: Cell proliferation along vascular islands during microvascular network growth, *BMC Physiol*. 2012;12:7.
- [82] Yang M, Aragon M, Murfee WL: Angiogenesis in mesenteric microvascular networks from spontaneously hypertensive versus normotensive rats, *Microcirculation*. 2011;18:574-582.
- [83] Murfee WL, Rappleye JW, Ceballos M, Schmid-Schonbein GW: Discontinuous expression of endothelial cell adhesion molecules along initial lymphatic vessels in mesentery: the primary valve structure, *Lymphat Res Biol*. 2007;5:81-89.
- [84] Fukushi J, Makagiansar IT, Stallcup WB: NG2 proteoglycan promotes endothelial cell motility and angiogenesis via engagement of galectin-3 and alpha3beta1 integrin, *Mol Biol Cell*. 2004;15:3580-3590.
- [85] Adams RH, Alitalo K: Molecular regulation of angiogenesis and lymphangiogenesis, *Nat Rev Mol Cell Biol*. 2007;8:464-478.
- [86] Alitalo K, Tammela T, Petrova TV: Lymphangiogenesis in development and human disease, *Nature*. 2005;438:946-953.

- [87] Furness JB: Arrangement of blood vessels and their relation with adrenergic nerves in the rat mesentery, *J Anat.* 1973;115:347-364.
- [88] Sandvig A, Berry M, Barrett LB, Butt A, Logan A: Myelin-, reactive glia-, and scar-derived CNS axon growth inhibitors: expression, receptor signaling, and correlation with axon regeneration, *Glia.* 2004;46:225-251.
- [89] Marko SB, Damon DH: VEGF promotes vascular sympathetic innervation, *Am J Physiol Heart Circ Physiol.* 2008;294:H2646-52.
- [90] Bearden SE, Segal SS: Microvessels promote motor nerve survival and regeneration through local VEGF release following ectopic reattachment, *Microcirculation.* 2004;11:633-644.
- [91] Bearden SE, Segal SS: Neurovascular alignment in adult mouse skeletal muscles, *Microcirculation.* 2005;12:161-167.
- [92] Gu XH, Terenghi G, Kangesu T, Navsaria HA, Springall DR, Leigh IM, Green CJ, Polak JM: Regeneration pattern of blood vessels and nerves in cultured keratinocyte grafts assessed by confocal laser scanning microscopy, *Br J Dermatol.* 1995;132:376-383.
- [93] Furness JB, Marshall JM: Correlation of the directly observed responses of mesenteric vessels of the rat to nerve stimulation and noradrenaline with the distribution of adrenergic nerves, *J Physiol.* 1974;239:75-88.
- [94] Zawicki DF, Jain RK, Schmid-Schoenbein GW, Chien S: Dynamics of neovascularization in normal tissue, *Microvasc Res.* 1981;21:27-47.
- [95] Creedon D, Tuttle JB: Nerve growth factor synthesis in vascular smooth muscle, *Hypertension.* 1991;18:730-741.
- [96] Zettler C, Rush RA: Elevated concentrations of nerve growth factor in heart and mesenteric arteries of spontaneously hypertensive rats, *Brain Res.* 1993;614:15-20.
- [97] Eichmann A, Makinen T, Alitalo K: Neural guidance molecules regulate vascular remodeling and vessel navigation, *Genes Dev.* 2005;19:1013-1021.
- [98] Norrby K, Franzen L: A tissue model for the study of cell proliferation in vitro, *In Vitro.* 1980;16:31-37.
- [99] Nehls V, Drenckhahn D: Heterogeneity of microvascular pericytes for smooth muscle type alpha-actin, *J Cell Biol.* 1991;113:147-154.

- [100] Nicosia RF, Nicosia SV, Smith M: Vascular endothelial growth factor, platelet-derived growth factor, and insulin-like growth factor-1 promote rat aortic angiogenesis in vitro, *Am J Pathol.* 1994;145:1023-1029.
- [101] Murakami T, Suzuma K, Takagi H, Kita M, Ohashi H, Watanabe D, Ojima T, Kurimoto M, Kimura T, Sakamoto A, Unoki N, Yoshimura N: Time-lapse imaging of vitreoretinal angiogenesis originating from both quiescent and mature vessels in a novel ex vivo system, *Invest Ophthalmol Vis Sci.* 2006;47:5529-5536.
- [102] Zhu WH, Iurlaro M, MacIntyre A, Fogel E, Nicosia RF: The mouse aorta model: influence of genetic background and aging on bFGF- and VEGF-induced angiogenic sprouting, *Angiogenesis.* 2003;6:193-199.
- [103] Bruyere F, Melen-Lamalle L, Blacher S, Roland G, Thiry M, Moons L, Franken F, Carmeliet P, Alitalo K, Libert C, Sleeman JP, Foidart JM, Noel A: Modeling lymphangiogenesis in a three-dimensional culture system, *Nat Methods.* 2008;5:431-437.
- [104] Stapor PC, Azimi MS, Ahsan T, Murfee WL: An angiogenesis model for investigating multicellular interactions across intact microvascular networks, *Am J Physiol Heart Circ Physiol.* 2013;304:H235-45.
- [105] Anderson CR, Hastings NE, Blackman BR, Price RJ: Capillary sprout endothelial cells exhibit a CD36 low phenotype: regulation by shear stress and vascular endothelial growth factor-induced mechanism for attenuating anti-proliferative thrombospondin-1 signaling, *Am J Pathol.* 2008;173:1220-1228.
- [106] Norrby K: In vivo models of angiogenesis, *J Cell Mol Med.* 2006;10:588-612.
- [107] Song JW, Munn LL: Fluid forces control endothelial sprouting, *Proc Natl Acad Sci U S A.* 2011;108:15342-15347.
- [108] Bayless KJ, Kwak HI, Su SC: Investigating endothelial invasion and sprouting behavior in three-dimensional collagen matrices, *Nat Protoc.* 2009;4:1888-1898.
- [109] Anghelina M, Moldovan L, Moldovan NI: Preferential activity of Tie2 promoter in arteriolar endothelium, *J Cell Mol Med.* 2005;9:113-121.
- [110] Kelly-Goss MR, Sweat RS, Azimi MS, Murfee WL: Vascular islands during microvascular regression and regrowth in adult networks, *Front Physiol.* 2013;In Press.

BIOGRAPHY

Peter Conrad Stapor was born August 6, 1986 and grew up in Herndon, Virginia. He received a Bachelor of Science in Biomedical Engineering from The University of Virginia in 2008 where he was a member of the Chi Phi Fraternity and UVA Rugby Club. In the fall of 2008, he began graduate studies at Tulane University in the Department of Biomedical Engineering to investigate microvascular dynamics. His work highlighted links between the microvascular and neural systems, characterized a new marker of pericytes with functional implications during angiogenesis, and established the rat mesentery culture model as a tool to investigate angiogenesis.

